USDOT Region V Regional University Transportation Center Final Report

NEXTRANS Project No. 0102IY04

Dynamic Multi Modal Multi-Objective Intersection Signal Priority Optimization

By

Eric Lo

Masters Candidate

University of Illinois at Urbana Champaign

ericlo2@illinois.edu

And

Juan C. Medina

Postdoctoral Research Associate

University of Illinois at Urbana Champaign

jcmedina@Illinois.edu

And

Rahim F. Benekohal (PI)

Professor

University of Illinois at Urbana Champaign

rbenekoh@illinois.edu

Report Submission Date: December 31, 2013

DISCLAIMER

Funding for this research was provided by the NEXTRANS Center, Purdue University under Grant No. DTRT07-G-005 of the U.S. Department of Transportation, Research and Innovative Technology Administration (RITA), University Transportation Centers Program. The contents of this report reflect the views of the authors, who are responsible for the facts and the accuracy of the information presented herein. This document is disseminated under the sponsorship of the Department of Transportation, University Transportation Centers Program, in the interest of information exchange. The U.S. Government assumes no liability for the contents or use thereof.

Dynamic Multi-Modal Multi-Objective Intersection Signal Priority Optimization

Introduction

In recent years travelers have shown an increased interest in multi-modal transportation including transit, bike, and pedestrian modes. However, traditionally traffic signal timing has mainly focused on efficiently serving a single mode (cars). In addition, public agencies have increased their support for mass transit ridership and expansion of bicycling and walking facilities to attract more users. So, traffic signal timing strategies should consider multi-modal perspectives that may require multi-attribute approaches leading to more environmentally conscious and sustainable policies.

Past research have studied various aspects of multi-modal traffic signal strategies, including the assessment of relative mode importance, and how to provide more equitable service for all modes by optimizing signal settings at intersections and along corridors. Most studies on the subject show multi-modal signal control is limited to at most two modes, and are based on traditional approaches, which are very restricting in nature compared to cycle-free strategies such as the one proposed in this study.

This project takes into account some of the concepts used in previous research, and applies multi-attribute decision-making (MADM) methods to combine the effects of four modes of transportation (automobiles, buses, pedestrians, and bicycles) in selecting the most appropriate signal timing settings at an intersection. Three MADM methods were used: SAW (Simple Average Weighting), AHP (Analytic Hierarchy Process), and TOPSIS (Technique for Order Preference by Similarity to Ideal Solution). The results from the MADM methods are compared for different scenarios, including scenarios with weights to specify the relative importance of the four modes. A case study involving an intersection with the option of servicing pedestrians using standard parallel crossings or a pedestrian scramble phase is evaluated.

In addition to the MADM methods, a multi-agent approach based on reinforcement learning was applied to optimize signal timings using a computer simulation package and real-time decision making based on inputs from virtual detectors. This resulted in a signal timing operation that is cycle-free and adaptive. The agent-based approach uses model-free reinforcement learning to optimize the operation of the signals through a multi-objective reward function. The agents make decisions, observe, and learn from the behavior of the system, evolving the knowledge about the scenario presented to the agent and thus, improving future decisions. The microscopic simulator VISSIM was selected for this study because it is capable of simulating all four modes of transportation: pedestrians, bicycles, motor-vehicles, and transit, and it also has the capabilities of using external controllers (i.e. reinforcement learning agents with a multi-objective reward function) for manipulating the traffic signals in running time.

Findings

Results indicate that all three methods selected signal timing settings that followed general expectations in terms of cycle length and green time splits; however, their optimal alternatives were not always the same. The sensitivity of the solutions also varied across strategies, with SAW and TOPSIS being more sensitive than AHP.

SAW and TOPSIS are well-suited for optimal selection of multi-modal signal timing parameters because they can deal with multiple criteria (modes of transportation and their characteristics) and large number of alternatives with simplicity. In TOPSIS, the utility of each mode is assumed to linearly increase or decrease across the range of alternatives, thus special consideration should be given to non-linear functions. While SAW considers each alternative separately, TOPSIS uses all alternatives together to normalize their utility, therefore a more careful and comprehensive selection of alternatives is required.

On the other hand, AHP allows inputs based on qualitative and quantitative comparisons between alternatives or modes, but it requires an extensive number of pairwise comparisons for problems with large number of alternatives. Matrix manipulations may also be an issue if many alternatives are considered at a given time. However, the method is less subject to variation when the reliability of the input data is questionable and when the alternatives are not evenly distributed across the utility range.

In terms of the agent-based strategy to control the signals, results showed that the agent effectively balanced delays for all modes and was sensitive to changes in the demands. Green times, and therefore cycle length, was very stable for the direction with low traffic (N-S) which had a very high lower bound that exceeded the time required to process motorized traffic, but was required for the pedestrians to complete the crossing. In contrast, green times in the E-W direction showed great variability and tried to balance the demands as they entered the links and the competing traffic. In this direction green times varied from its lowest possible value (18 seconds) to more than 100 seconds.

Average delays and number of stops per mode obtained with the agent-based approach confirmed that the green time variations responded to variability in the demand, since the delays were relatively stable for all replications once a performance plateau was reached. Overall, the agent-based approach showed potential for multi-modal applications and it is appealing since it reacts in real time to changes in the traffic conditions of all modes.

Overall, the agent-based approach showed potential for multi-modal applications and it is appealing since it reacts in real time to changes in the traffic conditions of all modes.

Recommendations

Further research is recommended to extend the analysis of MADM methods for multimodal traffic control. The relative ease of computation of these methods, combined with proven

performance in other domains, make this approach worth additional exploration. Results from this study support the potential application of these methods as an alternative to more traditional approaches.

The lack of guidelines to make the decision of providing or not a scramble phase (pedestrian exclusive phase) calls for further research in this matter. Sensitivity charts illustrate examples when a scramble phase is beneficial for all modes combined. However, additional analysis of multiple configurations and scenarios are needed to develop strong guidelines that are practice-ready.

Further studies on parameter selection and alternative algorithms are needed to strengthen the resources available to researchers and practitioners, and to generate stronger guidelines on how to use these types of cycle-free and adaptive strategies in a real world intersection. Additional research is also recommended to include a multimodal analysis along a corridor and in networks with closely-spaced intersections, where coordination of green times between adjacent signals is important.

Contacts

For more information:

Professor Rahim F. Benekohal
University of Illinois at Urbana Champaign
205 N Mathews Ave
Urbana, IL, 61801
Phone number: 217-244-6288
Fax number: 217-333-1924
Email Address: rbenekoh@illinois.edu

NEXTRANS Center
Purdue University - Discovery Park
2700 Kent B-100
West Lafayette, IN 47906

nextrans@purdue.edu
(765) 496-9729
(765) 807-3123 Fax

www.purdue.edu/dp/nextrans

NEXTRANS Project No. 0102IY04

Dynamic Multi Modal Multi-Objective Intersection Signal Priority Optimization

By

Eric Lo

Masters Candidate

University of Illinois at Urbana Champaign

ericlo2@illinois.edu

And

Juan C. Medina

Postdoctoral Research Associate

University of Illinois at Urbana Champaign

jcmedina@Illinois.edu

And

Rahim F. Benekohal (PI)

Professor

University of Illinois at Urbana Champaign

rbenekoh@illinois.edu

Report Submission Date: December 31, 2013

Contents

1 INTRODUCTION

In recent years travelers have shown an increased interest in multi-modal transportation including transit, bike, and pedestrian modes. However, traditionally traffic signal timing has mainly focused on efficiently serving a single mode (cars). In addition, public agencies have increased their support for mass transit ridership and expansion of bicycling and walking facilities to attract more users. So, traffic signal timing strategies should consider multi-modal perspectives that may require multi-attribute approaches leading to more environmentally conscious and sustainable policies.

Past research have studied various aspects of multi-modal traffic signal strategies, including the assessment of relative mode importance, and how to provide more equitable service for all modes by optimizing signal settings at intersections and along corridors. Most studies on the subject shows multi-modal signal control limited to at most two modes, and are based on traditional approaches, which are very restricting in nature compared to cycle-free strategies such as the one proposed in this study.

One of the main goals of this project is to take into account some of the concepts used in previous research, and apply multi-attribute decision-making (MADM) methods to combine the effects of four modes of transportation (automobiles, buses, pedestrians, and bicycles) in selecting the most appropriate signal timing settings at an intersection. The results from the MADM methods are compared for different scenarios, including scenarios with weights to specify the relative importance of the four modes. The selected MADM methods are for the analysis are SAW, AHP, and TOPSIS, which have been successfully used in several domains for complex decision making problems.

In addition to the MADM methods, a multi-agent approach based on reinforcement learning (RL) was applied to optimize signal timings using a computer simulation package and real-time decision making based on inputs from detectors. This resulted in a signal timing operation that is cycle-free and adaptive. The agent-based approach uses model-free RL to optimize the operation of the signals through a multi-objective reward function. The agents make decisions, observe, and learn from the behavior of the system, evolving the knowledge about the scenario presented to the agent and thus, improving future decisions. The microscopic simulator VISSIM was selected for this study because it is capable of simulating all four modes of transportation: pedestrians, bicycles, motor-vehicles, and transit, and it also has the capabilities of using external controllers (i.e. RL agents with a multi-objective reward function) for manipulating the traffic signals in running time.

The analysis of the performance of the MADM methods and the RL approach was conducted based on a case study involving an intersection with the option of servicing pedestrians using standard parallel crossings or a pedestrian scramble phase.

The following chapter provides a general background on the formulations used for the delay estimations, and overviews of the MADM methods and the agent-based approach. In Chapter 3, past studies on multimodal optimization and reinforcement learning agents are briefly mentioned to provide a general sense of the current state of art and practice. Chapter 4 defines the methods and strategies to compute solutions with the MADM methods, including unit-based strategies, occupancy, and a combination of the previous two. Chapter 5 presents the case study site and the current conditions at the intersection, setting the ground for the description of the implementation of the MADM methods and the definition of the agent and its components in a multimodal problem, contained in Chapter 6. The results and analysis are included in Chapter 7, additional work on an introductory analysis of whether to implement a scramble or no scramble phase is presented in Chapter 8, and conclusions are presented in Chapter 9.

2 BACKGROUND

2.1 Delay and performance measure

2.1.1 HCM delay formulas

The 2010 version of the Highway Capacity Manual (HCM) provides guidance and formulas on calculating delay for all road user modes: automobiles, transit, bicycles, and pedestrians along facilities, segments, and at intersections.

The average delay experienced by vehicles (including passenger cars and trucks) that arrive in the analysis period is given by:

$$d = d_1 + d_2 + d_3$$

Where:

d = control delay (s/veh),

d_1 = uniform delay (s/veh),

d_2 = incremental delay (s/veh), and

d_3 = initial queue delay (s/veh).

Uniform delay (d_1) is the delay incurred due to random arrivals throughout a cycle. Assuming there is a single effective green period during a cycle and a single saturation flow rate during the analysis period,

$$d_1 = \frac{0.5C(1 - g/C)^2}{1 - [\min(1, X)g/C]}$$

Where:

C = cycle length,

g = effective green time for phase, and

$X = v/(c \times PHF)$ = volume-to-capacity ratio and PHF = peak hour factor.

The capacity, c, is found by the product of the green ratio of the phase and the adjusted saturation flow rate of the lane: $c = s \times g/C$. As presented in the HCM chapters 18 and 31, the adjusted saturation flow rate, s, is a product of eleven factors which adjust for bus blockage, heavy vehicles, right turning vehicles, pedestrian-bike interactions, parking, etc. which affects a base saturation flow rate of 1,900 passenger cars per hour per lane for a signalized intersection, $s = s_0 f_W f_{HV} f_g f_p f_{bb} f_a f_{LU} f_{RT} f_{LT} f_{Lpb} f_{Rpb}$ where the factors adjust for:

- $f_W = lane\ width$
- $f_{HV} = heavy\ vehicles$
- $f_g = grade$
- $f_p = parking\ movements$
- $f_{bb} = bus\ blockage$
- $f_a = area\ type$
- $f_{LU} = lane\ utilization$
- $f_{RT} = right - turns$
- $f_{LT} = left - turns$
- $f_{Lpb} = left - turns\ and\ pedestrian - bicycle\ interaction$
- $f_{Rpb} = right - turns\ and\ pedestrian - bicycle\ interaction$

The total delay (d_T) with the incremental queue accumulation method can be used to replace the standard d_1 equation for progressed traffic movements, movements with multiple green times, and movements with multiple saturation flow rates (e.g. protected-permitted left-turn movements, as stated in HCM. The expression for d_T is the following:

$$Q_i = Q_{i-1} - (s/3600 - q/N)t_{t_{d,i}} \geq 0.0$$

$$d_T = \frac{\sum_{i=1}^{n} 0.5(Q_{i-1} + Q_i)t_{d,i}}{qC}$$

Where

Q_i = queue size at end of interval i (veh),

q = arrival rate = v/3600 (veh),

s = saturation flow rate (veh/h/ln), and

$t_{d,i}$ = duration where arrival and saturation are constant (s).

The baseline delay (without initial queue) is calculated similarly to d_T but instead of $t_{d,i}$, $t_{t,i} = \min(t_{d,i}, Q_{i-1}/w_q)$ is used, where w_q is the queue change rate.

On the other hand, incremental delay (d_2) takes into account random cycle failures when demand exceeds capacity or when there is prolonged oversaturation throughout the analysis period:

$$d_2 = 900T\left[(X-1) + \sqrt{(X-1)^2 + \frac{8kIX}{cT}}\right]$$

Where

T = analysis period duration (h),

k = incremental delay factor, and

I = upstream filtering adjustment factor.

Finally, initial queue delay (d_3) includes any additional delay that results from the presence of unmet demand from before the analysis period:

$$d_3 = \frac{3600}{vT}\left(t_A \frac{Q_b + Q_e - Q_{eo}}{2} + \frac{Q_e^2 - Q_{eo}^2 - Q_b^2}{2c_A}\right)$$

Where

t_A = adjusted duration of unmet demand in the analysis period (h),

Q_b = initial queue at the start of the analysis period (veh),

Q_e = queue at the end of the analysis period (veh),

Q_{eo} = queue at the end of the analysis period when $v \geq c_A$ and $Q_b = 0$ (veh), and

c_A = average capacity (veh/h).

For bicyclists, delay is calculated using the uniform delay formula for automobiles with the exception that when calculating the capacity, the saturation flow rate of a bicycle lane is 2,000 bicycles/hr. For pedestrians, delay is calculated by the HCM by:

$$d_p = \frac{(C - g_{walk})^2}{2C}$$

Where

d_p = pedestrian delay (s/p),

C = cycle length (s),

g_{walk} = effective walk time for the phase, refer to HCM equations 18-55, 56, and 57 for variations based on the presence of signal heads or actuation.

2.1.2 HCM performance measure

One of the performance measures the HCM uses to express the quality of flow for an approach and intersection is the Level of Service (LOS). It is typically based on delay and/or volume-to-capacity ratio for the automobile mode, as seen in Table 2-1. For analysis of an approach or an intersection, only control delay is used to estimate LOS. For analysis of individual lane groups, both control delay and the volume-to-capacity ratio for that particular lane group are used (HCM, 18-5). For pedestrian mode, pedestrian delay, number of traffic lanes crossed, number of right- and left-turning vehicles, vehicle speed, and the presence of right-turn channelizing islands are used to calculate a perception LOS score as shown in Table 2-2 (HCM, 18-7). These other factors adjust for the volume of conflicting vehicle movements, vehicle speed, number of lanes crossed etc. For bicycle mode, width of the cross street, paved shoulders, through, and

bicycle lanes, demand flow rates of left turn, through, and right-turn vehicle movements, number of through lanes, and proportion of on-street parking occupied are used to find the LOS score.

Table 2-1 – LOS Criteria for automobile mode for an intersection

Control Delay (s/veh)	LOS by Volume-to-Capacity Ratio	
	≤ 1.0	> 1.0
≤ 10	A	F
> 10 and ≤ 20	B	F
> 20 and ≤ 35	C	F
> 35 and ≤ 55	D	F
> 55 and ≤ 80	E	F
> 80	F	F
Source: Highway Capacity Manual 2010 Exhibit 18-4		

Table 2-2 – LOS Criteria for pedestrian and bicycle modes for an intersection

LOS Score	LOS
≤ 2.00	A
> 2.00-2.75	B
> 2.75-3.50	C
> 3.50-4.25	D
> 4.25-5.00	E
> 5.00	F
Source: HCM 2010 Ex. 18-5	

2.2 Multi-criteria procedures

Multi-attribute decision making (MADM) is used to select, from a finite set, one or more "alternatives" or "options" given multiple "criteria" or "attributes" that contribute a "value" to each alternative. The criteria can sometimes be conflicting when some are beneficial to the decision and others are costly. The use of weights that are assigned to each criteria aid in determining which criteria are more important than others. Policy decisions often involve a set of different criteria and alternatives where one has to be chosen to satisfy an overall goal. The

objective of MADM methods is to enable a decision maker to choose an alternative given these assigned weights and values.

2.2.1 SAW

Simple Additive Weighting (SAW) is frequently cited as the most used method for MADM. It involves normalizing each value either through linear normalization (each value is divided by the maximum value in that criteria) or vector normalization (each value is divided by the norm, square root of the sum of the squares of all values across the criteria). Typically, linear normalization is used. (Yoon & Hwang) The score of each alternative is then obtained by the sum of the products of the respective weight of each criteria by the normalized value for each alternative. The higher the score, the higher it is ranked which means it is more preferred. When the units are the same, such as in this case where delay is being used in either seconds per unit or seconds per person, the method can be simplified without normalization and the weighted values can be summed directly (also known as the Weighted Sum Method). (Triantaphyllou et al). The score of each alternative (s_j) is calculated as the total weighted delay, which is simply the sum of the products of the volume, the delay per unit, and the weight of each mode. Since delay is to be minimized, lower scores are better. The general expression to estimate the scores is as follows:

$$s_j = \sum_i v_i d_{ij} w_i$$

2.2.2 AHP

Analytical Hierarchy Process (AHP) is another popular MADM method. Introduced by Thomas Saaty in 1971, it structures a decision into different levels of criteria and alternatives that contributes to an overall goal/objective. Relative importance between modes result from a matrix of dimension *I* x *I* (Matrix 1 in Figure 2-1) and the pairwise comparisons ($P_{i,i}$) between modes (Matrix Set A in Figure 2-1). Values for the comparisons are selected out of 9 possible levels (1 through 9) in the original scale proposed by Saaty (alternative scales are also

available), with reciprocals being used when the other mode is more important (1/2, 1/3…1/8, 1/9). Then, the eigenvector of the *I* x *I* matrix (x_{II}) is calculated to obtain the weight for each mode. The same process is repeated *I* times in matrices of size *J* x *J* with pairwise comparisons of alternatives (signal timings) with respect to a given criteria such as delay, where delays from each alternative are ranked against each other ($P^{i}_{j,j}$). The resulting eigenvectors (x_{ji}, each with *J* rows) are placed together in a matrix (*J* x *I*) (Matrix 2 in Figure 2-1) that is multiplied to the eigenvector of the criteria (with *I* rows) (Matrix 3 in Figure 2-1). The final vector contains the score (s_j) of each alternative. These are then sorted from highest to lowest, resulting in a ranking of the alternatives. (Zolfani & Antucheviciene, Mateo) Figure 2-1 shows a representation of the steps to calculate the scores (s_j) in AHP.

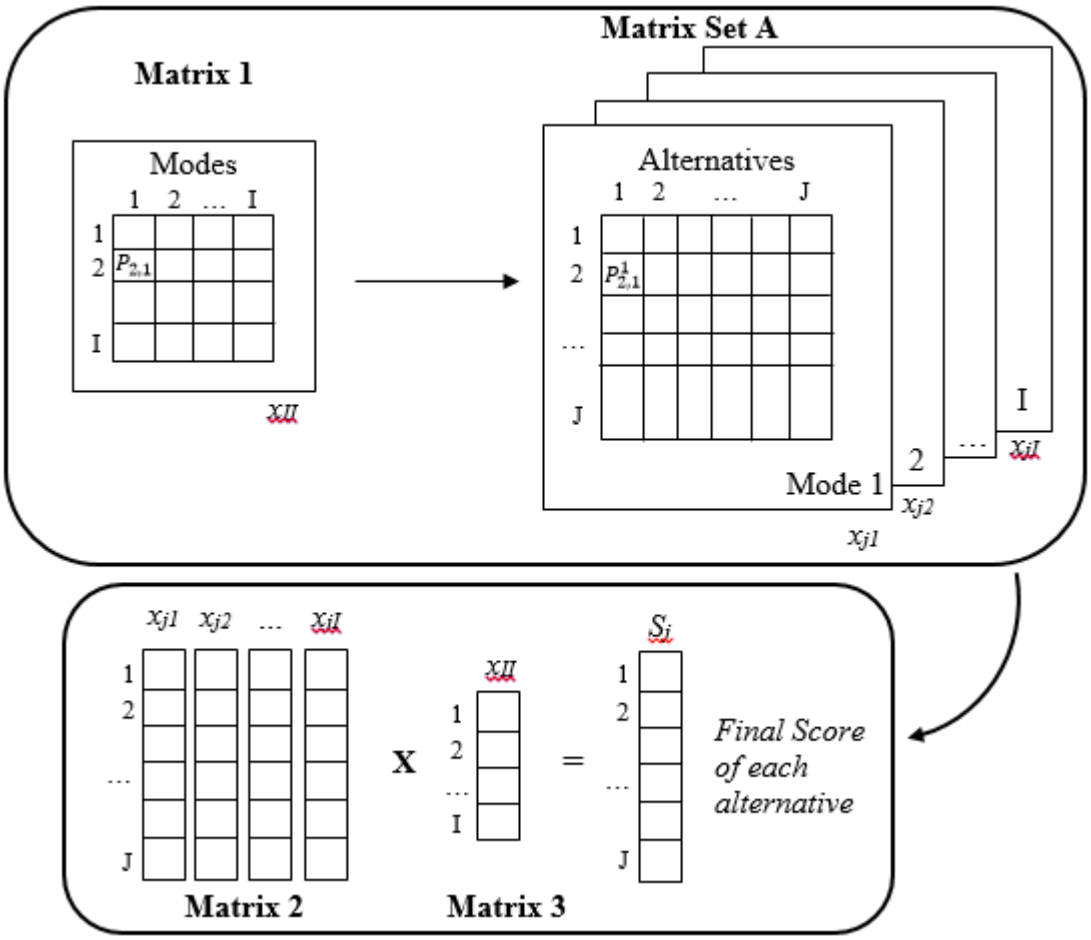

Figure 2-1 – Schematic representation of AHP

2.2.3 TOPSIS

Developed by Hwang and Yoon, TOPSIS ranks alternatives by viewing the decision as a geometric problem. The highest-ranked alternative (or ideal solution, IS) to be chosen should be closest to the most positive ideal solution (PIS) while being the furthest away from the most negative ideal solution (NIS). TOPSIS uses relative weights and the minimum and maximum values of each mode to determine the two ideal points (A^*, A^-) and the distances between each alternative and those points. By assuming that each criterion is monotonically increasing or decreasing in utility along with the use of geometric distances, it is a straightforward approach to ranking alternatives, and is the most sensitive method partially due to its reliance on the positive and negative extreme ideal points. (Mateo, Yeh). A schematic representation of TOPSIS is shown in Figure 2-2. First, each alternative (*j*) is evaluated for each mode (*i*) to obtain a rating (r_{ij}). In this implementation, ratings were the total delay experienced by a given mode when using a given alternative. Ratings are normalized (n_{ij}) (Matrix 1 in Figure 2-2) and multiplied by the corresponding mode weight (Matrix 2 in Figure 2-2) to obtain a matrix of weighted normalized values (w_{ij}) (Matrix 3 in Figure 2-2). In this paper, the mode weights were obtained from the eigenvector of the criteria matrix used in AHP (x_{II}). The distance of each alternative from the PIS and NIS is then calculated, resulting in a score. Higher scores are preferred.

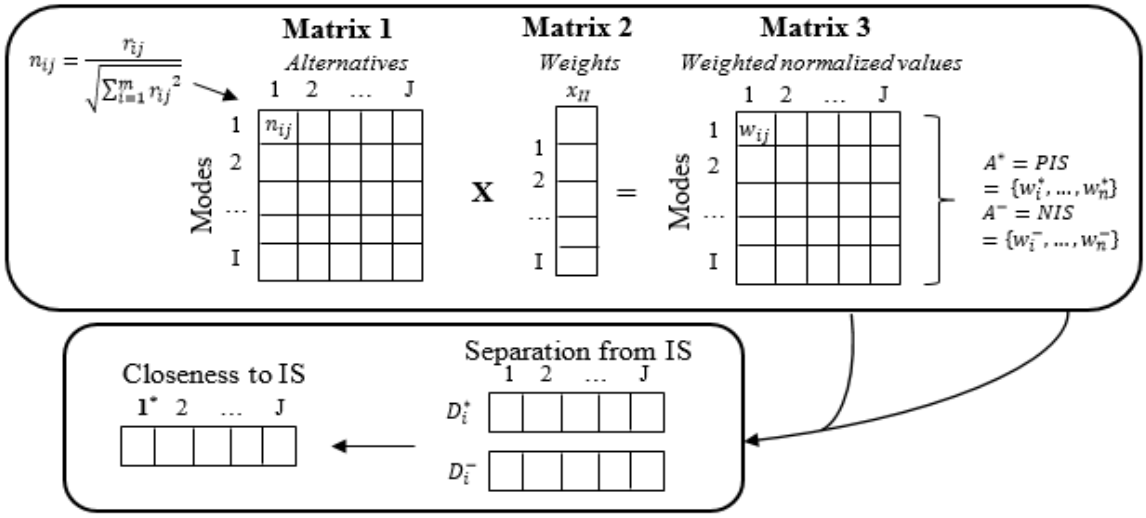

Figure 2-2 – Schematic representation of TOPSIS

2.3 Agent-based

An alternative approach to solve a multi-attribute decision making problem is the use of approximate tools incorporating artificial intelligence, and more specifically machine learning. Some complex problems may be difficult to model or may present difficulties for policy selection given uncertainties in the input values. Finding optimal signal timings at signalized intersections may fall into such category of complex problems if the variability in traffic and the ability to predict traffic behavior in the future is considered. Among several techniques from machine learning, reinforcement learning (RL) is well suited for this task given that it can adapt the system decisions in real time given actual traffic demands and it creates knowledge to develop an expert agent based on experience directly collected at the subject intersection. In other words, reinforcement learning has the potential to act as a human directing traffic in real time. Within reinforcement learning, Q-learning has been selected to be used as the mechanism for storing system knowledge, and thus for making decision and control the traffic signals.

In general a RL problem can be thought as the problem of finding the policy that guarantees maximum expected rewards $V^*(s)$:

$$V^*(s) = max_\pi V^\pi(s), for\ all\ s \in S$$

where $V^\pi(s)$ is the value of state *s* following policy π (also known as the "cost-to-go"), *x* is an action drawn from a finite set of possible actions. This maximization problem can also be described in terms of the value of state-action pairs (called Q-values), and therefore the goal will be to find a policy with action-value functions ($Q^\pi(s,a)$) leading to maximum expected total rewards:

$$Q^*(s,a) = max_\pi Q^\pi(s,a)$$

The advantages of having values of state-action pairs, as opposed of only states, are mostly observed in systems where the dynamics are not completely known (the algorithm is model-free) or where the random information received over time is not precisely determined in advance (such as the traffic signal problem). The reason for such advantage is that there is no need to estimate the full expectation of the transition function to perform an update of the Q estimates (as opposed to the standard Bellman equation). This is, in Q-learning:

$$\hat{q}(s,a) = c^{a}_{ss'} + \gamma \max_{a'} Q(s', a')$$

as opposed to the standard Bellman equation:

$$Q(s,a) = C^{a}_{ss'} + \gamma \sum_{s'} P^{a}_{ss'} \max_{a'} Q(s', a')$$

Where ($C_{ss'}$) is the cost to transition from *s* to *s'*, γ is a discount factor for the value of the next state $Q^{\pi}(s', a')$, and $P^{a}_{ss'}$ is the probability of transitioning to state *s'* given that the current state is *s* and the action taken is *a*.

Since the learning process is done gradually and based on experiencing sampled information from the system, the estimates can be updated using the following standard rule:

$$Q(s,a) = (1-\alpha)Q(s,a) + \alpha\hat{q}$$

where α is the learning rate.

The general algorithm for Q-learning can be formulated as shown in Figure 2-3.

1) Initialization:

$Q^0(s,x)=y$, y is and arbitrary value

2) While n episodes not finished:

Find initial state (s_0^n)

While episode not finished (t<T):

Select action x based on a given policy

Execute x, observe $c_{ss'}^x$, s'

Update: $Q_{t-1}^n(s,x) = (1-\alpha)Q_{t-1}^{n-1}(s,x) + \alpha(c_{ss'}^x + \gamma \max_{x'} Q_t^{n-1}(s',x'))$

Advance to next step: $s = s'$

Figure 2-3 – Pseudo-code for the Q-learning algorithm

Q-learning has shown good performance for a variety of practical problems under stationary conditions, even though the convergence of Q-values has only been proven if the states are visited an infinite number of times (Watkins, 1989, 1992). Arguably, this is because practical decision making does not require full convergence of Q-values as long as they are "sufficiently" different for the agent to commit to the best choice. Unfortunately, precise boundaries of the Q-learning algorithm for decision-making purposes only are not well defined and require further research.

Several researchers have used Q-learning for traffic control, and Q-learning is one of the most widely used RL techniques, but the applications have typically been limited to finding optimal policies for vehicular traffic, and not for multimodal purposes. This study uses Q-learning for multimodal traffic signal control as it is described in the following chapters.

3 LITERATURE REVIEW

3.1 Multimodal Analysis in HCM

HCM 2010 provides multimodal tools to analyze intersections by including automobiles, transit, pedestrians, and bicyclists into the analysis. However, despite it being a large advance in analyzing all modes that use an intersection as compared to previous editions, HCM 2010 has yet to treat the delay of users together. There is no overall method of combining delays; rather, it is segmented into delay or level of service (LOS) for each mode. In addition, the calculation of pedestrian delay is limited to a simple average of the red time that a user spends waiting and does not include the effect of volume or capacity, which the other modes do include.

3.2 Multimodal studies

The NCHRP Report 616 (2008) considers multi-modal levels of service and the interaction of car, bus, bicycles, and pedestrians in complete street designs so that they are taken into account in the design stage. The report provides references to several other studies analyzing LOS, but they do not discuss the timing of traffic signals from a multi-modal perspective. In addition, it does not combine LOS into a single comprehensive level of service, which leaves each mode fragmented and not comprehensive.

Christofa and Skabardonis (2011) formulated a traffic signal control system that would minimize total person delay at an intersection which considered user delays amongst passenger cars and buses but placed a greater emphasis on reducing the delays experienced by transit passengers. In particular, they developed a system which could be applied to Transit Signal Priority (TSP)

algorithms to make it take into account live conditions of transit vehicles which also had conflicting routes. After development of the system, they tested it with a mathematical program of a signalized intersection in Athens, Greece which had conflicting bus routes. The authors also point out that existing TSP only takes into account vehicle delay rather than person delay at an intersection. They compared results from the program under two scenarios – vehicle-based and person-based preferential treatment – versus a model of the existing signal settings. Their results indicated that their system improved total person delay at the intersection since it weighted the delays of transit vehicles higher (with an average occupancy of 40) than passenger cars (with an average occupancy of 1.25) and was able to take into account conflicting bus routes.

Fixed phases and cycle lengths were used, so that the only way to assign signal priority was to use early green or green extension. In addition, active signal priority was used since the model relied on the ability to sense traffic flow and transit vehicles, rather than passive signal priority, which relies on historical traffic data and expected bus frequency. Three scenarios were tested in their mathematical program – the base scenario with existing signal settings, one which minimized vehicle delay, and the other which minimized person delay. The results of their program with minimizing vehicle delay indicated that the car delay decreased by 3.81% but the transit delay jumped by 23.96%, resulting in a net increase in total delay of 3.63% for all users. However, when minimizing person delay was the goal, vehicle delay decreased by 1.11% and transit delay decreased by 19.97%, resulting in a net overall total delay decrease of 6.17% versus the existing signal settings. In general, the proposed optimization resulted in reduced person delays for all users for the modeled conditions. When comparing a person-based optimization against the vehicle-based optimization, the overall total delay at the intersection was modeled to be 9.5% less than a vehicle-based optimization. This was the result of comparing a worse scenario for transit users (vehicle-based optimization) to a better scenario (person-based) instead of to the base scenario (as manually calculated earlier). (Christofa and Skabardonis)

Taylor and Mahmassani (2010) considered bicycles along an arterial and their progression with fixed-timing plans. The authors' goal was to develop a conceptual framework for signal coordination for bicyclists by treating the problem as a multi-objective problem. Their objectives were to maximize one-way auto and bicycle progression while minimizing delay along a corridor and amongst the cross-streets and minimizing stops. They brought up challenges, which included the variations in speed due to users, effects of grade and wind, bandwidth, and ability to make left-turns under progression. They recommended educating bicyclists to maintain a higher than average speed to increase the likelihood of facing a green signal. Giving additional green time, more than needed by vehicles along the corridor, to bicyclists is also proposed for progression, even though it creates additional delay to cross-street autos. Lowering vehicle speeds is also suggested along with half-cycles. (Taylor and Mahmassani, 2010)

Shladover et al (2009) studied the speeds and behaviors of bicyclists while crossing wide arterials from a minor street. By doing so, they recommended the length of extended green intervals for minor streets when bicyclists are present so that they have sufficient time to cross. They believed that having them use actuated signals like pedestrians would be an inconvenience so it was important for there to be an accurate minimum green time, representative of a realistic crossing time, on the minor street to be in effect all the time so bicyclists are not trapped in the intersection (they noted that the current minimum green time was 4 sec).

They collected and analyzed startup time, free flow/cruising speed in the intersection, effects of road geometry and user demographics (most importantly, age), and the impacts of decreased green split for the major road. They recorded video images of two intersections with high bicyclist traffic in California (arterial: seven lanes, 40mph, and four lanes, 25 mph) and concurrent with the signal head. Using video image-processing software, they plotted the locations of bicyclists across the intersection overlaid with the traffic signal phase times. By doing so, they were able to obtain startup time, crossing time, and average speed of the

bicyclist. They also tested the effects of reducing green time for the arterial in VISSIM by increasing the minimum green for the side street and they found the effects to be minimal. In the end, they devised a crossing time estimate as a function of an offset time, width, crossing speed, and a factor. (Shladover et al, 2009)

Rouhieh (2008) and Alecsandru et al. (2010) analyzed a method to give an optimal coordinated signal plan along an urban arterial in Montreal for automobiles, bicyclists, and pedestrians. They adapted a "Delay-Safety" performance measure previously developed by Zhang and Prevedouros which applies a delay and safety factor per mode into a weighted average of traffic volume. They then use an Artificial Neural Network model to choose the best signal timing to optimize delay and safety. They used VISSIM along with traffic data from a newly installed bicycle lane at a one-way major arterial along four intersections in Montreal, Quebec. The model anticipates whether or not signal synchronization, and the characteristics of it, is most suitable given a set of inputs. Their results showed that 99.8% of the tested scenarios correctly identified which type of signal plan should be used (i.e. isolated, coordinated to promote automobiles, or coordinated to promote bicycles) which would give the optimal Delay-Safety value.

Noland (1996) argued for greater emphasis on pedestrians when it came to signal timing and to be treated more equitably in urban intersections instead of only favoring vehicular traffic. He said pedestrians' value of time is more costly than an automobile due in part to walking speed and the greater delay incurred because of the greater likelihood of encountering an unfavorable pedestrian signal. In particular, he recommended minimizing travel time costs for both cars and pedestrians. His optimization model relates the cost of travel delay from signal timings for drivers and pedestrians, where the optimal cost is the minimum of the sum of the product of the average delay, time value, and volume of each mode for automobiles and pedestrians. He made an assumption, based on studies, that a pedestrian waiting at a signal is twice as costly as a driver waiting in a car. Noland used a car occupancy of 1 in his analysis. His results from using his optimization formula generated costs per person for various cycle

lengths. It indicated that if the pedestrian-to-automobile volume ratio is larger than 3, then there should be longer green time allocated from a cycle for pedestrians to minimize total costs at the intersection. (Noland, 1996)

Carsten et al (1998) pointed out that often times pedestrian delay was 10 times vehicular delay in the UK, with minimum green times less than the average crossing time for pedestrians. In addition, they noted that the balance between pedestrian and vehicular traffic was not decided solely on economic or engineering studies, but it is also a political decision from a given jurisdiction. Their implementation of a pedestrian detection and actuated pedestrian phase was met with resistance from authorities who were worried it might lead to unacceptable vehicular delay. (Carsten et al, 1998)

Virkler (1998) examined the benefits of considering pedestrians in signal coordination and later Bhattacharya and Virkler (2005) balanced delays to both vehicles and pedestrians by modifying signal timings and offsets between intersections in a network. They used the value of time as the indicator of delay, which AASHTO described as a function of average hourly family income, and any delay that is produced by the model is converted into a monetary value, and use Noland's optimization equation of minimizing the total cost x average delay x volume. Various offsets of 5-second multiples were analyzed along with a 15-second walk signal, resulting in an average vehicle occupancy of 1.22 passengers per vehicle. The authors simulated five coordinated intersections with two-way traffic in Synchro with existing pedestrian and vehicle delay data. They then compared which offsets created the minimum delay between the two modes. Their results showed that traffic signal progression which didn't take into account pedestrian speeds ended up increasing overall network delay. (Bhattacharya and Virkler, 2005)

The HCM formula for pedestrian delay, as provided earlier, treats pedestrian delay only as a function of the average amount of time they wait per cycle, or the effective red time. Unlike the other modes, the effect of demand and capacity of the crosswalk facility is not taken into account, which may reduce the accuracy of the delay estimates. According to the HCM

formula, if there are a large number of people waiting to cross the street, someone who arrives behind that group/platoon even when the "Walk" indication is on would not experience any delay at all.

A formula which represents the area in between the arrival and saturation curves as presented by Dion et al (2004) for vehicular delay was used to simulate pedestrian delays. This formula includes saturation flow rate and arrival flow rates to help acknowledge that shortcoming and it represents the delay experienced per user per cycle. The model assumes uniform arrival and departures and provides results for the average delay incurred by a vehicle or pedestrian per cycle as shown in the expression below. (Dion et al, 2004)

$$d = \frac{r^2}{2C}\left(\frac{s}{s-v}\right)$$

Where

d = delay (s/user/cycle),

r = effective red (s),

s = saturation flow rate (user/s), and

v = arrival flow rate (user/s).

Ishaque and Noland (2005) furthered research on providing more equitable treatment of pedestrians at an intersection compared to the traditional approach of giving vehicles priority. They decided to use the microsimulator VISSIM instead of using analytical methods. A four-intersection network was simulated with midblock pelican crossings (pedestrian-actuated signals) and zebra crossings (yield to pedestrians when they are present). Five vehicle types were simulated – car, pedestrian, taxi, heavy vehicle, and bus, where bus and heavy vehicles were equated into two cars. Bus lanes were also present and vehicle and pedestrian flows were provided. A key difference in their assumptions is their treatment of pedestrians as no-interaction types, where their movements are not subject to any other nearby presence instead of "modeling of pedestrians as vehicles… allows all waiting pedestrians to proceed simultaneously when the pedestrian green phase starts."

Eight cycles ranging from 45 to 120 seconds were tested and pedestrian green time was kept at 8 seconds. The simulation was run until a specified convergence criteria is met. Two vehicle phases (one for each road direction) were input for each of the four intersections. They also analyzed the differences of single and double pedestrian phases for 104- and 120-second cycles. Single pedestrian phase is when pedestrians are served after two vehicle phases, whereas double pedestrian phase is when pedestrians are served after each vehicle phase. Various flow multipliers were tested from 1.0 (free-flow) to 1.9 (overcapacity) for sensitivity purposes. Their principal finding was that a cycle between 60 and 72 seconds was optimal for light traffic conditions and 90 seconds for heavier. In addition, in their simulated network, double pedestrian phases reduce vehicle throughput with 104- and 120-second cycles compared with a conventional 60-second cycle with a single pedestrian phase. The value of time per mode is factored into another analysis. They included a scramble crossing, yet their model does not allow for diagonal movements. (Ishaque and Noland, 2005)

3.3 Agent-based

Specifically for traffic signal control, the study of reinforcement learning dates back about 15 years ago. One of the first of such studies was completed by Thorpe (1997), using the RL algorithm SARSA to assign signal timings to different traffic control scenarios. Later, Wiering (2000) discussed a state representation based on road occupancy and mapping the individual position of vehicles over time, and Bakker (2005) later extended this representation using an additional bit of information from adjacent intersections. This allowed communication between agents, trying to improve the reward structure and ultimately the overall performance of the system.

Using a different approach, Bingham (1998, 2001) defined fuzzy rules to determine the best allocation of green times based on the number of vehicles that would receive the green and red indication. He presented a neural network to store the membership functions of the fuzzy rules,

reducing memory requirements. It is noted that a Cerebellar Model Articulation Controller (CMAC) has also been used in the past to store the information learned (Abdulhai, 2003). Another application using fuzzy rules for traffic control was presented by Appl and Brauer (2000), where the controller selected one of the available signal plans based on traffic densities measured at the approaching links. Using a single intersection, their fuzzy controller outperformed learning from a controller with a prioritized sweeping strategy.

Choy et al. (2003) also used a multi-agent application for traffic control, but creating a hierarchical structure with three levels: intersection, zones, and regions. The three types of agents (at each level) made decisions based on fuzzy rules, updated their knowledge using a reinforcement learning algorithm, and encoded the stored information through a neural network. Agents selected a policy from a set of finite possible policies, where a policy determined shortening, increasing, or not changing green times. Experiments on a 25-intersection network showed improvements with the agents compared to fixed signal timings, mostly when traffic volumes were higher.

Campoganara and Kraus (2003) presented an application of Q-learning agents in a scenario of two intersections next to each other, showing that when both of those agents implemented the learning algorithm, the systems performed significantly better than when only one of none of them did. The comparison was made with a best-effort policy, where the approach with longer queue received the green indication.

A study on the effects of non-stationary nature of traffic patterns using RL was proposed by De Oliveira et al. (2006), who analyzed the performance of RL algorithms upon significant volume changes. They pointed out that RL may have difficulties to learn new traffic patterns, and that an extension of Q-learning using context detection (RL-CD) could result in improved performance.

Ritcher et al (2007) showed results from agents working independently using a policy-gradient strategy based on a natural actor-critic algorithm. Experiments using information from adjacent intersections resulted in emergent coordination, showing the potential benefits of communication, in this case, in terms of travel time. Xie (2007) and Zhang (2007), explored the use of a neuro-fuzzy actor-critic temporal difference agent for controlling a single intersection, and used a similar agent definition for arterial traffic control where the agents operated independently from each other. The state of the system was defined by fuzzy rules based on queues, and the reward function included a linear combination of number of vehicles in queue, new vehicles joining queues, and vehicles waiting in red and receiving green. Results showed improved performance with the agents compared to pre-timed and actuated controllers, mostly in conditions with higher volumes and when the phase sequence was not fixed.

Most of the previous research using RL focused on agents controlling a single intersection, or a very limited number intersections interacting along an arterial or a network. However, with an increase in the interest of RL techniques for traffic signal control, some recent studies have explored to use of reward functions specifically derived from the traffic domain and with consideration of queue spillovers in oversaturated conditions. Examples of these studies are those by El-Tantawy and Abdulhai (2010) and Medina, Hajbabaie, and Benekohal (2012 and 2013).

Regarding multimodal applications using RL, efforts in previous research have been focused on multimodal transportation in the sense of accounting for multiple types of vehicular traffic including passenger cars, trucks, and automobiles. However, to the authors' knowledge, there is no published work related to multimodal traffic signal control incorporating the effects of non-motorized traffic, namely pedestrians and bicycles. This study presents one of such applications, weighing the time spent by four modes of transportation (passenger cars, buses, bicycles, and pedestrians) to improve traffic signal control in a true multimodal approach based on Q-learning.

4 METHODOLOGY

The general objective of the methodologies used in this study was to minimize delay for all users of the four modes at an intersection. A number of different approaches can be followed to take into account delays for different modes at a signalized intersection, including methodologies that obtain intersection delay or LOS per mode, and methodologies that consider delay per direction per mode. The delay per mode takes the average delay per mode and multiplies it by the volume to obtain the total delay. This treats users from all approaches as having the same average delay, which can result in an unfair treatment for a particular direction with higher delay. An alternative approach is delay per direction per mode, which takes the sum of each delay per lane group/direction and multiplies it by the volume in that lane group/direction. This is a more accurate portrait of the total delay experienced at the intersection for uneven demands, which when combined with delays from other modes, allows a more fair comparison to be made. Both approaches to estimate delay are evaluated for all three MADM methods (SAW, AHP, and TOPSIS):

- Approach 1: Average delay "Per Mode" x {volume of that mode}
- Approach 2: ∑ Delay "Per Direction" per mode x {volume of that mode in that direction}

In addition, three strategies were used to combine delays from the different modes of transportation, as described in the following sections.

4.1 Strategies

4.1.1 Unit-based

The traditional strategy for obtaining the delay at an intersection can be referred to as unit-based delay. This strategy counts each "moving unit" as a singular element that, on average,

experiences the same delay as other moving units using the intersection, including cars, buses, bikes, and pedestrians. Since delay is typically calculated based on the characteristics of a passenger car, a mode such as a transit vehicle has to be accounted for in a different way. A bus can be counted as two passenger car equivalent units, where the conversion can be due to factors such as the greater space it occupies or its slower acceleration rate versus a passenger car. In this sense, buses are responsible for twice the delay of a car at an intersection. Bicycles and pedestrians are also counted as one moving unit each. The delays for these modes are calculated separately except for buses, which would incur twice the average delay of a car. The overall average intersection delay based on units would be estimated as the average delay that each mode experiences weighted by the number of units per mode:

$$Total\ intersection\ delay\ (unit-based) = d_{Car} \cdot Vol_{Car} + d_{Bus} \cdot Vol_{Bus} + d_{Bike} \cdot Vol_{Bike} + d_{Ped} \cdot Vol_{Ped}$$

where $d_{Bus} = BC \cdot d_{Car}$, $BC = Bus\ Conversion\ factor$, and the summation uses either of the aforementioned approaches.

4.1.2 Occupancy

Although heavy vehicles such as buses can be converted into passenger car equivalents, the delay of all users in the bus may not be of equitable proportion. For instance, if a bus is treated as two passenger cars to allow for volume and delay calculations to be done, in the end, it would mean that it experiences only twice the delay a car experiences. In a majority of cases especially in urban areas, this would be highly unrepresentative of the actual delay incurred on the bus due to the larger person capacity it can hold as compared to a passenger car. A typical passenger car might hold up to five people but a typical bus can hold ten times as much.

A way of more equitably expressing the delay experienced by different vehicular modes at an intersection is by applying an occupancy factor to the calculation to give results in person delay. Studies have looked at this as a way of giving extra consideration to buses over cars when there

are heavy mass transit usage or traffic control measures such as transit signal priority. This method multiplies the control delay by the average occupancy by the respective volume of each mode. While cars may have an average occupancy of 1.25 persons per car, a bus can have an average occupancy of 10 people per bus. Each passenger on the bus experiences the same delay and twice the delay of a passenger car. This is a more accurate representation of the genuine delay that a bus has than using the typical unit-based approach. Bicyclists and pedestrians would have an occupancy of 1. The total occupancy delay would be the sum of the delays multiplied by the volume and the occupancy, whether using the average delay per mode multiplied by total volume or sum of the delay per direction multiplied by volume per direction.

$$Total\ intersection\ delay\ (occupancy - based) = (d_{Car} \cdot Vol_{Car} \cdot Occ_{Car}) + (d_{Bus} \cdot Vol_{Bus} \cdot Occ_{Bus}) + (d_{Bike} \cdot Vol_{Bike} \cdot Occ_{Bike}) + (d_{Ped} \cdot Vol_{Ped} \cdot Occ_{Ped})$$

4.1.3 Mode Priority and Occupancy

Importance weights can also be applied to reflect an agency's decision to prioritize one mode over another. This is applied to the control delay per vehicle by multiplying the importance for each mode by the volume and occupancy of each mode. This allows for a higher priority to be given to modes based on a mode's value of time, socioeconomic conditions or environmental considerations. For instance, if cars are given an importance weight of 1 as a baseline, buses can be given a higher weight, to reflect its ability to serve more people efficiently and reduce congestion. Pedestrians and bicyclists can be given a greater weight than cars since their value of time might be higher. Priority weights can be assigned directly or found using AHP.

$$Total\ intersection\ delay\ (priority - based) = (d_{Car} \cdot Vol_{Car} \cdot Occ_{Car} \cdot Pri_{Car}) + (d_{Bus} \cdot Vol_{Bus} \cdot Occ_{Bus} \cdot Pri_{Bus}) + (d_{Bike} \cdot Vol_{Bike} \cdot Occ_{Bike} \cdot Pri_{Bike}) + (d_{Ped} \cdot Vol_{Ped} \cdot Occ_{Ped} \cdot Pri_{Ped})$$

5 CASE STUDY

The intersection of Green St and S Wright St, located at the border of the cities of Urbana and Champaign, Illinois was chosen as the case study to test the MADM methods and the agent-based approach. The intersection is at a unique location since east of it lies the campus of the University of Illinois at Urbana-Champaign, and west of it lies what is referred to as "Campustown." The campus side has multiple buildings, residential and dining halls, and the Illini Union, a focal point for students and administrative offices. Campustown is a downtown area with shops, restaurants, and private housing located primarily along Green St. Northeast of the intersection is home to engineering buildings, southeast to the Illini Union and the remainder of the campus, southwest is Campustown which eventually turns into the south side of the campus, and the northwest is Campustown which eventually turns into private residential housing. The east-west direction has heavy vehicular and pedestrian volume due to its respective attractions.

The intersection geometry of Green and Wright St composes of four approaches with varying lane configurations and widths, as seen in Figure 5-1. The eastbound approach consists of one shared through and right-turn lane and a left turn lane, with one wide receiving lane (approximately 18 ft). The westbound approach consists of one left-turn lane, one through lane, and one right-turn lane, with one receiving lane. The northbound approach consists of one shared left, through, and right-turn lane, with one receiving lane. The southbound approach consists of one shared left-turn and through lane, with one receiving lane. No right-turns are allowed from the southbound approach. A parking lane is located upstream and downstream of the southbound approach. Bus stops are located downstream of the northbound and eastbound approaches. Sidewalk curb extensions (aka bumpuots or

neckdowns) are installed at the northeast, southwest, and northwest corners to increase waiting area to accommodate pedestrians. All sidewalk corners have a higher radius of curvature than the northwest corner. Due to the asymmetrical nature of this geometry, not all pedestrian crossings intersect the curb cut or other crosswalks at a 90° angle. Markings are also present for diagonal crossings for pedestrians for a scramble crossing. On-street bicycle lanes are provided only along the northbound approach on the east side of S Wright St; an off-street lane is provided on the westbound approach on the north side of Green St.

Figure 5-1 – Satellite view of intersection (Google Maps)

The current phasing plan for the intersection consists of three vehicular phases and one pedestrian phase and is pre-timed with no actuation (Table 5-1). The east-west phase has 31 seconds of green with permitted left-turns, followed by three seconds of yellow and two seconds of all-red. Next, the southbound phase consists of nine seconds of protected green and yellow for the left-turn and through traffic. Northbound traffic then receives a green phase concurrently with the southbound phase for nine additional seconds of green followed by three seconds of yellow and two seconds of all-red. Finally, a pedestrian scramble phase begins with seven seconds of Walk, 21 seconds of Flashing Don't Walk, and three seconds of all-red. The

cycle length is 90 seconds. The abbreviated forms of approaches used hereafter are "EB" for eastbound, "WB" for westbound, "NB" for northbound, and "SB" for southbound. Movements and lane groups are abbreviated as "L" for left-turn, "T" for through, and "R" for right-turn.

Table 5-1 – Existing phasing plan

Phase	Approach	Movements Allowed	Duration (s)
1	EB	LTR	31 (green), 3 (yellow), 2 (all-red)
	WB	LTR	
2	SB	LT	9 (green)
3	NB	LTR	9 (green), 3 (yellow), 2 (all-red)
	SB	LT	
4	Pedestrian	Scramble	7 (Walk), 21 (Flashing Don't Walk), 3 (all-red)
		Total	90

Nine bus lines run through the intersection:

- 1 Yellow: runs along Wright St
- 2 Red: runs west along Green St and turns right onto Wright St (and reverse)
- 4 Blue: runs along Wright St
- 5 Green: runs along Green St
- 9 Brown: runs along Wright St
- 12 Teal: runs west along Green St and turns right onto Wright St (and reverse)
- 13 Silver: runs north along Wright St and turns right onto Green St (and reverse)
- 22 Illini: runs north along Wright St and turns right onto Green St (and reverse)
- 27 Air Bus: runs north along Wright St and turns right onto Green St (and reverse)

Table 5-2 shows hourly vehicular volumes collected on a weekday when classes were in session separated by approach and vehicle type: car or bus. Trucks were not included in this count.

Table 5-2 – Hourly vehicular volumes

	Car			Bus		
	Left	Through	Right	Left	Through	Right
EB	47	198	10	0	2	0
WB	24	256	72	10	4	7
NB	1	5	3	0	10	11
SB	52	25	3	5	12	0

Pedestrian counts were performed by placing a video camera by the window on the second floor of a retail store at the northwest corner. Due to the limitations of the viewing angle of the camera, counts for pedestrians were only obtained on three of the six crossings at the intersection: the north crosswalk (crossing Wright St), east crosswalk (crossing Green St), and one of the diagonals (crossing northwest corner to/from southeast corner). Although pedestrian volumes could have been obtained for the other crosswalks by counting the number are within view, it would not be accurate since their exact location stepping on/off would be unknown.

In addition, these counts were done as part of a study to determine the speed between free-flow and non-free-flow pedestrians and between individuals and groups, with combinations of the four, at an intersection with a pedestrian scramble phase. Due to the varying paths that pedestrians can take from one curb cut to the other, as well as the presence of diagonal crosswalks, each crossing direction was segmented into different starting and stopping channels. The channels were based on the location of the existing crosswalk lines but could be extended based on preliminary observation on where pedestrians queued and/or left the curb. The distance of these path combinations that could be taken at each crossing was measured. Since the channels of where pedestrians were stepping off and on the curb at the southwest corner was outside of the viewing angle of the camera, counts of those subjects would not be useful.

Therefore, to represent the pedestrian volumes at the crosswalks that were not counted, the volumes of their counterparts were assumed as their volumes. For example, the north crosswalk volumes would equal the south crosswalk volumes, the east volumes would equal the west volumes, and the northwest-southeast diagonal volumes would equal the northeast-southwest diagonal volumes. A summary of the counts is in Table 5-3.

Table 5-3 – Pedestrian volumes for scramble phase

Crosswalk	Volume (p/h)
North (real)	284
South (assumed)	284
East (real)	73
West (assumed)	73
Northwest-Southeast diagonal (real)	251
Northeast-Southwest diagonal (assumed)	251

6 IMPLEMENTATION

6.1 Operations

The experiment includes calculations for two modes of operation at the intersection: no-scramble and scramble. No-scramble is defined to be normal operation where pedestrians are given a Walk and Flashing Don't Walk indications during the same vehicular green phase in the same direction. When a conflicting movement is given the green, these pedestrians would see the steady Don't Walk indication. Scramble is defined to be where pedestrians are given the steady Don't Walk indication during all vehicular movement phases. They only receive the Walk and Flashing Don't Walk indications during their own special phase, where vehicles are not allowed to move. This is not to be confused by the presence of parallel and diagonal crosswalks, where parallel crosswalks allow for pedestrians to cross at a generally perpendicular angle to the opposite side of the street, whereas diagonal crosswalks allow pedestrians to cross opposite corners. During a scramble mode, bicyclists were assumed to not move and to follow vehicular green.

For scramble mode, since no pedestrian movements are permitted, a time of six seconds was assigned as the minimum green time for each vehicular phase. For no-scramble mode, in order to determine the minimum green times needed to accommodate the Walk and Flashing Don't Walk indications, the average of the path lengths for each crosswalk were first obtained. If path lengths were not available because they were not included in the previously mentioned study, then a straightforward measurement between midpoints of each crosswalk were used. The maximum of each pair of parallel crosswalks (e.g.: maximum of east (65 ft) and west (36 ft) and maximum of north (44 ft) and south (39 ft) was then used to calculate the Flashing Don't Walk times by dividing the distance by the walking speed (Table 6-1). The walking speed used

for the pedestrian clearance interval is defined to be 3.5 feet per second by the Manual on Uniform Traffic Control Devices. (MUTCD, 497) The minimum Walk indication was determined by using HCM equation 18-66 (or equivalently HCM equation 31-72), which calculates the timing required to serve pedestrian demand per cycle:

$$t_{ps} = 3.2 + \frac{L}{S} + 0.27N_{ped}$$

Where

$t_{ps} = pedestrian\ service\ time\ (s)$,

$L = crossing\ length\ (ft)$,

$S = walking\ speed\ (ft/s), and$

$N_{ped} = pedestrian\ flow\ rate\ (peds/hr)$.

The minimum vehicular green time for a no-scramble mode would then be the Flashing Don't Walk added to the Walk time of five seconds (Table 6-2).

To simplify the simulation of the experiment as well as remove concerns regarding the storage length of the left-turn bay when high volumes are involved and in the delay calculation of permitted left-turns, left-turns volumes were removed (Table 6-3). Including protected left-turn phases for each approach would have led to minimum cycle lengths of 70 seconds for base undersaturated volumes, 80 seconds for saturated volumes, and 90 seconds for oversaturated volumes. Since the current signal operation has a 90 second cycle length, this would have reduced the reasonable ranges of alternatives. In addition, bicycle lanes were assumed to be on-street so that they would be complying with traffic signals meant for automobiles.

Table 6-1 – Experiment timing plan for pedestrians

Mode:	No-scramble		Scramble	
Direction	Walk	Flashing Don't Walk	Walk	Flashing Don't Walk
EB, WB	Varies by volume	13 s	-	-
NB, SB	Varies by volume	19 s	-	-
Scramble	-	-	Varies by volume	24 s

Table 6-2 – Experiment phasing plan

Phase	Approach	Movements Allowed	Minimum Green (No-scramble)	Minimum Green (Scramble)	Change and Clearance
1	EB	TR	18 s	6 s	4 s
	WB	TR			
2	NB	TR	24 s	6 s	4 s
	SB	T			
3	Pedestrian	-	-	-	1 s (scramble only)

Table 6-3 – Experiment vehicular volumes

	Car			Bus		
	Left	Through	Right	Left	Through	Right
EB	0	198	10	0	2	0
WB	0	256	72	0	4	7
NB	0	5	3	0	10	11
SB	0	25	3	0	12	0

Because the current phasing plan has a scramble phase for pedestrians, no volumes were available for parallel crosswalks. To include this in the delay calculations when in a parallel crossing mode, assumptions were made so that the total diagonal volumes were divided between the four crosswalks equally and added to the parallel volumes (Table 6-4). The total diagonal volumes were not split according to demand weighted by the existing parallel crosswalks since it is unknown exactly how pedestrians would use the intersection if diagonal crossings were not present.

Table 6-4 – Experiment pedestrian volumes for parallel phases

Crosswalk	Volume (p/h)
North (assumed)	409
South (assumed)	409
East (assumed)	199
West (assumed)	199

6.2 Delay estimation

The effective green time for each phase was equal to the green time for each lane group since the lost times and extensions canceled each other out with the current assumed change and clearance times.

As mentioned earlier, the adjusted saturation flow rate, *s*, for a lane group is a function of the product of the base saturation flow rate, 1900 pc/h/ln, and eleven adjustment factors. The following assumptions were made in calculating *s* for all lane groups:

- $f_W = lane\ widths\ in\ range\ of\ 10\ ft - 12.9 ft \rightarrow 1.00$
- $f_{HV} = heavy\ vehicles\ assumed\ to\ be\ 0 \rightarrow 1.00$
- $f_g = grade\ assumed\ to\ be\ level \rightarrow 1.00$
- $f_p = no\ parking\ is\ present \rightarrow 1.00$
- $f_{bb} = buses\ not\ blocking\ flow\ in\ lane\ group\ w/i\ 250\ ft\ of\ stop\ line \rightarrow 1.00$
- $f_a = not\ a\ CBD \rightarrow 1.00$
- $f_{LU} = only\ one\ shared\ or\ exclusive\ lane\ per\ lane\ group \rightarrow 1.00$
- $f_{RT} = adjustment\ for\ right\ turns: see\ below$
- $f_{LT} = f_{Lpb} = no\ left\ turns \rightarrow 1.00$
- $f_{Rpb} = right - turn\ pedestrian - bicycle\ adjustment: see\ below$

The adjustment for right turns for a lane group that does not share itself with another movement (e.g. through or left) is: $f_{RT} = \frac{1}{E_R}$, where $E_R$is the equivalent number of through cars for a protected right-turning vehicle = 1.18. The only lane group that meets this criteria is the WBR (westbound right) lane group. The resulting equation would be $s = s_0 \cdot f_{RT} \cdot f_{Rpb} \cdot 1.00$. If a lane group involves shared right-turn and through movements, a different approach is used which involves HCM Equation 31-61 and its supporting equations:

$$s_{sr} = \frac{s_{th}}{1 + P_R(E_{R,m} - 1)}$$

Where

s_{th} = saturation flow rate of an exclusive through lane (adjusted for lane width, heavy vehicles, grade, parking, buses, and area type),

P_R = proportion of right-turning vehicles in the shared lane (decimal), and

$E_{R,m}$= modified through-car equivalent for permitted right-turning vehicles.

Supporting equations:

$$E_{R,m} = \left(\frac{E_R}{f_{Rpb}} - 1\right) P_{lc} + 1$$

$$P_{lc} = 1 - \left(\left[2\frac{v_{app}}{s_{lc}}\right] - 1\right)^2 \geq 0.0$$

$$v_{app} = \frac{v_{lt} + v_{th} + v_{rt}}{N_{sl} + N_t + N_{sr}}$$

Where

P_{lc} = probability of a lane change among the approach through lanes,

v_{lt}, v_{th}, v_{rt} = demand flow rate of left-turn, through, and right-turn lane groups for approach,

N_{sl}, N_t, N_{sr} = number of lanes in shared left-turn and through, through, and shared right-turn and through lane group, and

s_{lc} = maximum flow rate at which a lane change can occur = $3{,}600/t_{lc}$ where $t_{lc} = 3.7\ s$.

The adjustment for right-turn pedestrian-bicycle, f_{Rpb}, is calculated to reduce the saturation flow rate due to interaction between pedestrians in the crosswalk, bicyclists in the bicycle lane, and right-turning automobiles. If there is a no-scramble mode, then only bicyclists are included and if there is a scramble mode, then both pedestrians and bicyclists are included.

Pedestrians:

$$v_{pedg} = v_{ped}\frac{C}{g_{ped}} \leq 5{,}000$$

Where

v_{pedg} = pedestrian flow rate during the pedestrian service time (p/h),

v_{ped} = pedestrian flow rate in the subject crossing (in both directions) (p/h), and

g_{ped} = pedestrian service time; if not actuated = effective green time of phase (s).

If $v_{pedg} \leq 1{,}000$, then the pedestrian occupancy $OCC_{pedg} = \frac{v_{pedg}}{2000}$. Otherwise, $OCC_{pedg} = 0.4 + \frac{v_{pedg}}{10000} \leq 0.90$.

Bicycles:

$$v_{bicg} = v_{bic}\frac{C}{g} \leq 1{,}900$$

$$OCC_{bicg} = 0.02 + \frac{v_{bicg}}{2{,}700}$$

Where

v_{bicg} = bicycle flow rate during the green indication (bicycles/h),

v_{bic} = bicycle flow rate (bicycles/h),

g = effective green time of phase (s), and

OCC_{bicg} = bicycle occupancy.

To combine both modes, the relevant conflict zone occupancy, OCC_r, is:

$$OCC_r = \left(\frac{g_{ped}}{g} OCC_{pedg}\right) + OCC_{bicg} - \left(\frac{g_{ped}}{g} OCC_{pedg} OCC_{bicg}\right)$$

In this experiment, the number of receiving lanes is equal to the number of turn lanes, so Equation 31-81 is used to calculate the occupied time, $A_{pbT} = 1 - OCC_r$. This is also equal to f_{Rpb}. This is then used to calculate the adjusted saturation flow rate.

For this experiment, the peak hour factor was assumed to be 1.0, period of analysis $T = 0.25\,hr$, the incremental delay factor $k = 0.5$, and the upstream filtering adjustment factor, $I = 1.0$. An initial queue of zero vehicles in all lane groups was assumed. Since the bicycles are traveling in on-street bike lanes, they are expected to respect the green signal for their direction and to not move into the intersection at all other times. Therefore, their effective green time is equal to the effective green time for their phase.

For pedestrian delay, the formula provided by Dion is adopted to represent the average delay per person in a crossing per cycle. The saturation flow rate for pedestrian movements, s, was calculated by using the HCM section on pedestrian circulation facility capacity. Pedestrian capacity can be expressed in terms of unit flow or pedestrians per minute per foot of walkway width. For a corner at a crosswalk with crossing directions, the capacity is given as 23 peds/min/ft. (HCM, 4-32) It was assumed based on average measurements of the holding area that 10 ft of width was available. This was then converted into seconds to result in $s = 3.833\ ped/s$. For the given intersection, for a parallel crossing, there are four crosswalks and two cardinal directions per crosswalk, resulting in eight movements. For a scramble crossing, there are six crosswalks resulting in 12 movements. The green time that is used is equal to the Walk indication, since they assume that pedestrians will stop entering the crosswalk during that time.

When pedestrians who normally are able to cross diagonally due to a scramble phase are forced to cross in a two-stage parallel crossing, they incur in additional delay. This delay is a result of the additional wait time on the sidewalk and time needed to cross the additional distance. These were taken into account by adding to the pedestrian delay formula an average delay that is incurred based on the time until the Walk indication for the second crossing.

6.2.1 Analytical approach with multi-criteria methods

The analytical approach involves the use of C++ programming in Microsoft Visual Studio. The above inputs and delay equations were coded to follow a routine which calculates delays and LOS per lane group, per mode, and an overall average delay for the intersection, weighted by volume, for signal time combinations between a user-selected minimum and maximum cycle length at discrete cycle length increments. The input volumes for all modes can be adjusted for varying volumes to result in adjusted volumes. The conversion of buses to passenger car equivalents is also performed. Saturation flow rates are calculated for each lane group. If a lane group involves right-turns, this is recalculated later for each signal time combination.

The minimum vehicular green times stated earlier in Table 6-2 are used in determining the boundaries of signal timings for vehicles for each cycle. The program first starts off with calculations under the no-scramble mode. It then begins with the minimum green time for the east-west direction and the remaining time available for the north-south direction is calculated based on lost times (yellow and all-red times), with a minimum green time for that direction as well. During a no-scramble mode, these times would be reflective of the minimum Walk (5 s) and Flashing Don't Walk times for that particular direction. During a scramble mode, these minimum times would be 6 s. Once a signal time setting has been established, delays and LOS are calculated.

The goal of the routine is to then store the intersection delays for unit-based, occupancy-based, and priority-based and check for the minimum intersection delay for each method. If the current intersection delay is lower than the currently-stored minimum, then this new result along with the signal timing associated with it, are stored. The results are output into a file. The routine then advances an additional second for the east-west direction while subtracting a second from the north-south direction. When the self-checking mechanism has exhausted itself in allowable combinations for one cycle length, it moves to the next cycle increment. When the allowable combinations in the maximum cycle length is reached, the program will redo the entire process but for the scramble mode. If there are no pedestrians present, then the program will not enter the scramble mode.

Results were then verified with the commercial traffic analysis software *HCS 2010 Streets* developed by McTrans to check the validity of calculations. The delays for unit-based, occupancy-based, and priority-based were then used in the SAW, AHP, and TOPSIS methods, with the previously mentioned weights and rankings then applied. SAW is automatically obtained through the choice of minimum intersection delay, weighted by volumes for each mode, from the program.

6.2.2 Agent-based approach

As mentioned above, in addition to MADM methods, an approach using artificial intelligence in the form of reinforcement learning (RL) was also used to generate a multimodal control policy. Q-learning was the RL chosen for this application and its implementation in the context of multimodal optimization is presented in this section.

The basic structure of the RL system was previously presented by Medina et al (2013), and consists of an independent agent on each intersection to be analyzed. In this particular scenario only one intersection is considered, thus the communication module is not required, but it is noted that the system can be scaled to multiple intersections and to network configurations if needed.

The case study was modeled in the traffic simulator VISSIM, which allowed the use of a user-defined signal controller and the manipulation of the traffic signals in real-time.

As it is shown in Figure 6-1, the agent's internal structure is composed of the following elements: a module to read inputs and perceive the state of the system, set or pool of potential actions to choose from, a reward function, a method to update the estimates and the current value of state-action pairs, and a method for action selection.

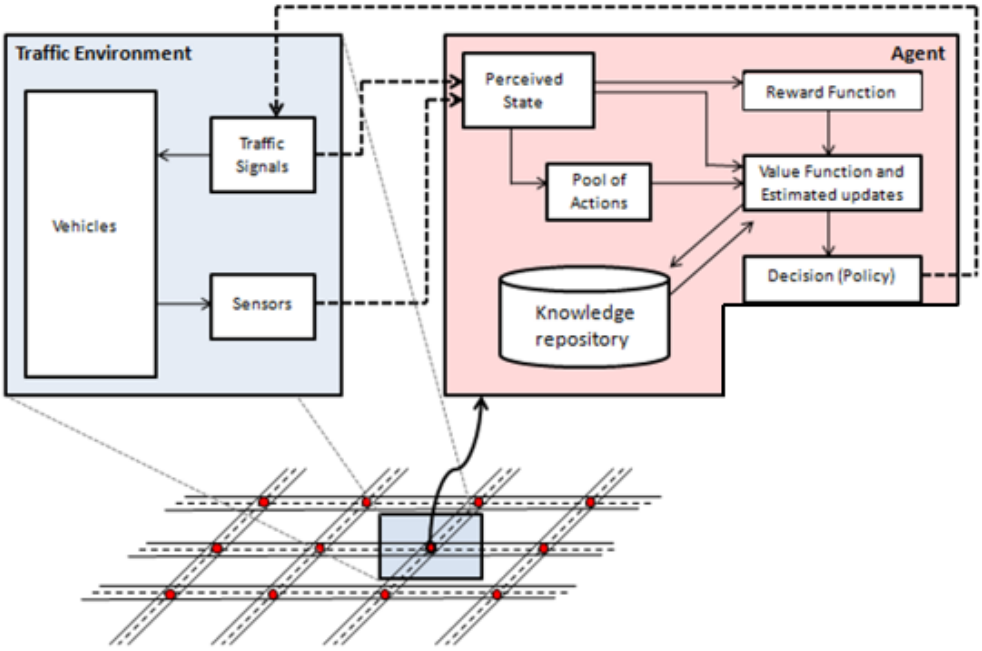

Figure 6-1 – Schematic representation of RL agent and the environment

It is noted that since the Q-learning algorithm is used, the agent can learn an optimal policy regardless of the action selection policy, as long as there is an adequate balance between exploration and exploitation such that all state-action pairs are visited with enough frequency. More details on the action selection scheme are provided below.

A description of each of the elements embedded in the agent is given as follows:

6.2.2.1 Input

The agent perceives the current state of the system by means of standard information available to traffic controllers about motorized vehicles and the state of the traffic signals. For this multimodal application, information on pedestrians and bicycles were also gathered in real time by means of detectors placed on the bike paths and sidewalks, in a similar way that motorized vehicles are typically detected through the use of inductive loops.

Thus, the inputs for the agent consisted of the current state of the signals and calls from advance and stop bar detectors for motorized vehicles, bicycles, and pedestrians. These allowed the agent to estimate the current queue and therefore the demand from each of the modes.

Individual calls from each detector for each moving unit (a car, a bicycle or a pedestrian) are received by the agent and used to create a perception of the state of the system. A representation of the current state (S) is created using the following structure:

$$S = \{v_{ew}, v_{ns}, b_{ew}, b_{ns}, p_{ew}, p_{ns}\ , g\}$$

Where v_{ew} is the current state of vehicles in the east-west direction, v_{ns} is the current state of vehicles in the north-south direction, and g represents the signal displaying the green indication; the remaining elements represent the state of bicycles in the two directions of traffic (b_{ew}, b_{ns}), and the state of pedestrians also in the two directions of traffic (p_{ew}, p_{ns}).

The state space may grow to a value greater than desired if each of the elements has a wide range of possible values. A number of solutions can be implemented so solve this situation, including merging values from different modes, for example merging motorized vehicles and bicycles, or narrowing the range of values each element can take.

6.2.2.2 Action Set

A set of possible actions was limited to modifications to the state of the traffic signals given the restriction of a minimum green time once a phase is initiated. Since the case study did not consider left-turning phases, only two signal phases in no-scramble mode were allowed: east-west and north-south. Different scenarios may include any number of phases, and restrictions on the phase sequence may or may not be imposed to the agent to analyze cases ranging from

total sequence freedom, to partial restrictions (e.g. leading left turns), to fixed sequence. Therefore, only two actions were available: give the right of way to E-W or to N-S. Decisions were taken by the agent every 2 seconds, which is the same frequency that new data was obtained from the environment.

6.2.2.3 Reward function

One of the most important aspects of the agent definition is the reward function. Rewards indicate the immediate benefits of taking an action, and are used for updating the long-term values of state-action pairs (i.e. Q-values) and drive the knowledge gathered by the agent.

For the agent to learn a given reward signal and to include it efficiently in its knowledge, it is ideal to express the rewards in terms of the state variables. Thus, if a reward signal is closely associated with the perceived state of the system, the agent can have a better estimation of the value of that state the next time it is visited.

Rewards can be defined based on any number of calculations once the current state of the system is identified. In this research, the goal was to provide the agent flexibility for treating different transportation modes with a given importance weight and being able to account for their quality of service separately. Thus, the reward function combines components from all four modes to estimate their individual pressure to obtain the green indication.

The basic expression for the reward estimation had two main components. One component estimates the combined value of users from all modes that would benefit if the green indication is received in each direction, and the second component estimates the time losses if the current phase is terminated. The main reward expression is shown as follows:

$$Reward(\varphi) = Benefit(\varphi) - (I(\varphi) * Penalty)$$

$$Benefit(\varphi) = \sum_x w_x^g g_x^\varphi - w_x^r r_x^\varphi$$

$$Penalty = \beta_1 \frac{PhaseDuration + \beta_2}{PhaseDuration + \beta_3} + \beta_4 \sum_x w_x^p g_x$$

Where w_x^g and w_x^r are the weights assigned to mode *x* when it is receiving the green and red light indication, respectively; g_x^φ and r_x^φ are the states of mode *x* in the direction receiving the green and red light indication under the phase φ, respectively; $I(\varphi)$ is an indicator function that is equal to 1 if the phase φ is different from the current phase and 0 otherwise; β_i are positive coefficients, and w_x^p is the weight assigned to the current state of mode *x* for penalty purposes (or g_x).

The reward function considers basic aspects of signal control by implementing a penalty that increases with the phase duration, modeling the delay of users receiving the red indication. This guarantees that as long as there is demand in a given approach, the corresponding phase will eventually be initiated regardless of the opposing volume, preventing extremely long waiting times for low volume approaches.

Previous studies by the authors along corridors and in networks also account for the effects of long queues generating potential blockages upstream. Extensions to arterials and networks need to be carefully considered but are straightforward.

6.2.2.4 Knowledge update and storage

The agent incorporates information to its knowledge by adding the immediate reward obtained by the previous action. This is performed by weighting the immediate reward with past rewards from the same state-action pair using the standard Q-learning update form shown as follows:

$$Q(s,a) = (1-\alpha)Q(s,a) + \alpha\hat{q}$$

$$\hat{q}(s,a) = Reward + \gamma \max_{x'} Q(s',a')$$

Where $Q(s,a)$ is the value of the executing action a in state s; α is the learning rate that determines the tradeoff between immediate and long terms rewards; γ is the discount factor to represent the value of obtaining delayed rewards; and s' and a' are the state and action in the next time step.

Modifications to the standard rule have been made to account for the fact that there is a minimum phase duration. In cases where the agent attempts to change the phase before the minimum duration has elapsed, the agent will obtain a maximum Q value corresponding to taking the action that leads to the current phase. In this way, the agent always makes decisions and updates its knowledge, even if it is forced to continue the current phase.

6.2.2.5 Action selection scheme

A mechanism to select an action given the current estimates of the state (or state-action pairs) is necessary in order have an adequate spread in the number of states experienced, and also to visit them frequently enough to generate trusted estimates of their true value. Therefore, the action selection should consider the tradeoffs between maximizing immediate outcomes (exploitation) and the potential discovery of long-term benefits after suboptimal actions are taken in the short term (exploration).

The design of an adequate action selection strategy is even more significant for "off-policy" algorithms (such as Q-learning). This is because off-policy algorithms perform the learning process independent from the action selection process as long as states are eventually visited with "sufficient" frequency. A common approach for the action selection mechanism is the use

of an *e*-greedy policy, where the maximization of the immediate action is performed at all times, except for a random action selection with probability *e*.

Similarly, a probabilistic action selection using a Boltzman or soft max distribution is common practice. Under this scheme, exploration is performed more often in the early stages of the learning process, as indicated by the number of times a state has been visited, and is also dependent on the current estimations of the values of being in a state. The general form of the probability of selecting a given action can be expressed as follows:

$$p_x(a) = \frac{e^{\frac{Q(s,a)}{T}}}{\sum_{b \in A} e^{\frac{Q(s,b)}{T}}}$$

where T is a temperature factor that controls the probability of exploration versus exploitation and is dependent on the number of times a state has been visited. The greater the value of T, the more likely the agent is to have similar probabilities for all actions, and therefore to explore more often. Thus, each action has a probability to be chosen and it is a function of the estimated value of a state and the number of times the state has been visited.

On the other hand, a combination of different action selection mechanisms or a hybrid approach can also be adopted. In such implementations, action selection can be guided based on one strategy at early stages, but then modified when estimates are considered to be more stable. This was precisely the choice selected in this study where the following strategies were combined: a) the very first time a state is visited, the action selection is biased towards the approach with the higher combination of number of vehicles and the amount of time they have been in the link; b) If the agent arrives at a state that has already been visited, but it has not taken one particular action for the first time, the decision is biased to take that action as a means of forced exploration. This is done until all actions have been tried at least once; c) once all actions have been experienced, a proportional rule to choose the best action was

implemented using a Boltzman distribution, until the estimates were considered to be more stable; and d) at later stages in the training process, e-greedy selection was used to choose the action with the highest value estimates. This hybrid approach allowed for more extensive exploration at the beginning of the agent training, slowly transitioning to exploitation of higher state values as the estimates became more reliable.

7 RESULTS & ANALYSIS

This chapter presents the results and analysis of the three MADM methods (SAW, AHP, and TOPSIS) for selecting optimal signal timing settings given a known demand, and also the results from a reinforcement learning (RL) agent controlling the traffic signal based on real-time inputs and using Q-learning.

7.1 MADM Methods

For the analytical approach, when the routine was finished, the optimal solutions involved only the no-scramble mode signal timings. This is due to the increased delays it has on automobiles and bicycles based on the given volume inputs. The total delay and the average intersection delay, which was used as the comparison for finding the optimal signal timing, was consistently lower for the no-scramble mode (Table 7-1) than the scramble mode (Table 7-2) due to the presence of high car and pedestrian volume along the EW directions. For this reason, the analysis that was carried out for SAW, AHP, and TOPSIS used delays from the no-scramble mode. It should be noted that if concerns for pedestrian safety with turning vehicles were a deciding factor, then a scramble mode might be warranted as is currently implemented. In addition, both per mode and per direction delays, as described earlier, are provided.

Table 7-1 – Example of No-scramble per direction Unit-based delays

Cycle length:	60	60	60	60	60	60	60	60	60	60	60	60
Eff. green EB/WB:	18	19	20	21	22	23	24	25	26	27	28	29
Eff. green NB/SB:	34	33	32	31	30	29	28	27	26	25	24	23
Walk indication EW:	5	6	7	8	9	10	11	12	13	14	15	16
FDW EW:	13	13	13	13	13	13	13	13	13	13	13	13
Walk indication NS:	15	14	13	12	11	10	9	8	7	6	5	4
FDW NS:	19	19	19	19	19	19	19	19	19	19	19	19
SAW Unit delay (delay by dir*vol)												
Car	10592	9978	9418	8899	8415	7960	7530	7117	6720	6344	5988	5650
Bus	924	916	915	917	923	933	945	959	974	992	1013	1037
Bike	590	563	536	509	483	458	434	410	387	365	343	322
Ped	31228	30777	30347	29938	29549	29181	28833	28507	28200	27914	27649	27404
Total	43334	42235	41215	40263	39371	38532	37742	36993	36281	35616	34994	34414
Intersection (avg)	**22.56**	**21.99**	**21.45**	**20.96**	**20.49**	**20.06**	**19.65**	**19.26**	**18.89**	**18.54**	**18.22**	**17.91**

Table 7-2 – Example of Scramble per direction Unit-based delays

Cycle length:	60	60	60	60	60	60	60	60	60	60	60	60
Eff. green EB/WB:	6	7	8	9	10	11	12	13	14	15	16	17
Eff. green NB/SB:	17	16	15	14	13	12	11	10	9	8	7	6
Walk indication:	4	4	4	4	4	4	4	4	4	4	4	4
FDW:	24	24	24	24	24	24	24	24	24	24	24	24
SAW Unit delay (delay by dir*vol)												
Car	84663	54500	36474	26372	21011	18001	16092	14740	13701	12854	12138	11520
Bus	3906	3033	2521	2249	2126	2079	2069	2081	2108	2148	2203	2280
Bike	975	940	905	871	837	804	772	741	710	680	651	622
Ped	32169	32169	32169	32169	32169	32169	32169	32169	32169	32169	32169	32169
Total	121713	90642	72068	61660	56142	53053	51102	49730	48687	47851	47161	46591
Intersection (avg)	**63.36**	**47.18**	**37.52**	**32.10**	**29.23**	**27.62**	**26.60**	**25.89**	**25.34**	**24.91**	**24.55**	**24.25**

7.1.1 Analytical approach

The analytical approach involved using the delays output from the program and applying the SAW, AHP and TOPSIS ranking methods to come up with an optimal solution. This includes both per mode and per direction delays. The optimal solution for SAW comes directly from selecting the signal timing setting for a particular strategy (unit-, occupancy-, or priority-based) that has the lowest average delay for the intersection. For unit-based delays, the optimal timing for both per mode delay and per direction delay is a cycle length of 70 s with 39 s of green for the EW and 23 s of green for the NS directions (Table 7-3 and Table 7-4).

For occupancy-based delays, the optimal timing for per mode delay is a cycle length of 70 seconds with 39 s of green for EW and 23 s of green for NS whereas for per direction it is a cycle length of 60 s with 29 s of green for EW and 23 s of green for NS (Table 7-5 and Table 7-6). Since the NS direction is more heavily trafficked by buses and buses have an occupancy of 10 users per bus (330 bus users) vs the EW direction (130 bus users), the lower total delay had an impact as compared to unit-based and per mode delays. It also balanced out the delay experienced by car users, where the EW direction (670 car users) was greater than the NS (45 car users) by not giving more time to the NS. When occupancy was a factor, per mode and per direction delays chose different optimal timings, as lower cycle lengths meant less wait for the buses in the NS direction.

Similar results for priority-based delays are shown in Table 7-7 and Table 7-8. The weights that were applied for priority-based delays were a result of applying AHP to a comparison between the four modes (Figure 7-1 and Figure 7-2). The desire was to simulate a decision to make buses more important than other modes, but have bikes and pedestrians treated similarly. The low cycle lengths make sense due to the undersaturated conditions for automobiles (Table 7-3).

After the analysis with SAW, a set of ten signal timings alternatives were selected, including the optimal timing, for comparison with AHP and TOPSIS. These alternatives were chosen to

represent the following two cases: one where the times are equivalent for both directions (giving equal treatment), and another where the NS direction receives the minimum green time. These options are provided to simulate the choices that a decision maker could face in choosing the signal timings for multimodal operation without knowing detailed operational details.

In order to use the different weighting powers of AHP and TOPSIS, the delays for AHP and TOPSIS used the average delays per mode and per direction as representative values for each alternative (Table 7-9). AHP was applied in a similar fashion to how the weights for priority-based delays for SAW were obtained. Table 7-10 shows the inputs used in an AHP comparison to obtain the weights for unit-, occupancy-, and priority-based delay, with resulting weights for each strategy in Figure 7-4, Figure 7-6, and Figure 7-8.

Figure 7-9, Figure 7-10, Figure 7-11, and Figure 7-12 show the eigenvector from the pairwise comparisons of the ten signal timing alternatives for per mode delays, and if the per mode delays are used as weights, the final AHP rankings for each strategy are shown in Figure 7-13, Figure 7-14, and Figure 7-15. The optimal alternative was a timing of 80-49-23 in unit-, occupancy-, and priority-based strategies. The second best alternative was 70-39-23. For per direction delays, Figure 7-16, Figure 7-17, Figure 7-18, and Figure 7-19 show the eigenvector from the pairwise comparisons of the ten alternatives. After multiplying by the mode weights, the final AHP rankings for each strategy are in Figure 7-20, Figure 7-21, and Figure 7-22. Since the initial comparisons treated alternatives with lower delays as more preferable, the higher the eigenvalue for an alternative, the more preferred that alternative is compared to the others. The optimal alternative was a timing of 60-29-23 in unit-, occupancy-, and priority-based strategies. The second best alternative varied between 70-39-23 for unit- and occupancy-based delays and 60-26-26 for priority.

For TOPSIS, optimal timings varied between cycle lengths of 60 to 80 s for both per mode and per direction as shown in Figure 7-23 to Figure 7-28. This optimal choice was close to what

SAW and AHP picked in most cases, with it choosing the same alternative as SAW four out of six times. Its second choice was often the optimal alternative that another multi-criteria method picked. It should be noted that TOPSIS can be influenced by extreme values in alternatives, as this affects the ideal solutions and the distances of each alternative.

Summary tables and figures for increasing the volumes by three and four times to simulate saturated and oversaturated conditions, respectively, are provided in Appendix A. As the pedestrian volume increased, the minimum walk time needed also increased, and the minimum green time for the NS direction increased.

To summarize, the same set of operations are performed using three different multi-criteria methods. SAW weights each mode as 1, whereas AHP and TOPSIS weight according to volume for unit-based, volume x occupancy for occupancy-based, and volume x occupancy x priority for priority-based:

- SAW, AHP, TOPSIS
    - Unit-based
        - Per mode
        - Per direction
    - Occupancy-based
        - Per mode
        - Per direction
    - Priority-based
        - Per mode
        - Per direction

Table 7-3 – SAW Unit per mode and v/c ratios for Undersaturated

SAW-Unit-per mode				Optimal						
Timing	1	2	3	4	5	6	7	8	9	10
Scramble No [0]/Yes [1]:	0	0	0	0	0	0	0	0	0	0
Cycle length:	60	60	70	70	80	80	90	90	100	100
Effective green EB/WB:	26	29	31	39	36	49	41	59	46	69
Effective green NB/SB:	26	23	31	23	36	23	41	23	46	23
Walk indication for peds (no scramble) EW:	13	16	18	26	23	36	28	46	33	56
Walk indication for peds (no scramble) NS:	7	4	12	4	17	4	22	4	27	4
Total delay										
Car	6623	5756	7376	5402	8141	5282	8913	5302	9691	5416
Bus	1071	931	1193	873	1316	854	1441	857	1567	876
Bike	387	322	437	276	486	242	536	215	586	194
Ped	28200	27404	29180	27469	30301	28021	31516	28898	32797	30002
Intersection (avg)	18.89	17.91	19.88	17.71	20.95	17.91	22.08	18.36	23.24	18.99
X=v/c for EB_T:	0.245	0.220	0.240	0.191	0.236	0.174	0.233	0.162	0.231	0.154
X=v/c for EB_R:	0.028	0.023	0.027	0.018	0.026	0.016	0.026	0.014	0.025	0.013
X=v/c for WB_T:	0.321	0.287	0.314	0.249	0.309	0.227	0.305	0.212	0.302	0.201
X=v/c for WB_R:	0.241	0.197	0.231	0.156	0.224	0.135	0.219	0.122	0.215	0.113
X=v/c for NB_T:	0.030	0.034	0.030	0.040	0.029	0.046	0.029	0.051	0.029	0.057
X=v/c for NB_R:	0.048	0.056	0.047	0.070	0.046	0.086	0.045	0.103	0.044	0.124
X=v/c for SB_T:	0.060	0.067	0.058	0.078	0.057	0.090	0.057	0.101	0.056	0.112

Table 7-4 – SAW Unit per direction

SAW-Unit-per dir*vol by dir				Optimal						
Timing	1	2	3	4	5	6	7	8	9	10
Scramble No [0]/Yes [1]:	0	0	0	0	0	0	0	0	0	0
Cycle length:	60	60	70	70	80	80	90	90	100	100
Effective green EB/WB:	26	29	31	39	36	49	41	59	46	69
Effective green NB/SB:	26	23	31	23	36	23	41	23	46	23
Walk indication for peds (no scramble) EW:	13	16	18	26	23	36	28	46	33	56
Walk indication for peds (no scramble) NS:	7	4	12	4	17	4	22	4	27	4
Total delay										
Car	6720	5650	7478	4981	8250	4558	9029	4279	9814	4097
Bus	974	1037	1090	1295	1207	1579	1325	1880	1444	2195
Bike	387	322	437	276	486	242	536	215	586	194
Ped	28200	27404	29180	27469	30301	28021	31516	28898	32797	30002
Intersection (avg)	18.89	17.91	19.88	17.71	20.95	17.91	22.08	18.36	23.24	18.99

Table 7-5 – SAW Occupancy per mode

SAW-Occ-per mode*vol*occ				Optimal						
Timing	1	2	3	4	5	6	7	8	9	10
Scramble No [0]/Yes [1]:	0	0	0	0	0	0	0	0	0	0
Cycle length:	60	60	70	70	80	80	90	90	100	100
Effective green EB/WB:	26	29	31	39	36	49	41	59	46	69
Effective green NB/SB:	26	23	31	23	36	23	41	23	46	23
Walk indication for peds (no scramble) EW:	13	16	18	26	23	36	28	46	33	56
FDW for peds (no scramble) EW:	13									
Walk indication for peds (no scramble) NS:	7	4	12	4	17	4	22	4	27	4
FDW for peds (no scramble) NS:	19									
Total delay										
Car	8279	7195	9220	6753	10176	6603	11142	6628	12114	6770
Bus	10709	9307	11925	8735	13162	8541	14412	8573	15669	8757
Bike	387	322	437	276	486	242	536	215	586	194
Ped	28200	27404	29180	27469	30301	28021	31516	28898	32797	30002
Intersection (avg)	16.45	15.30	17.56	14.95	18.72	15.01	19.92	15.33	21.16	15.81

Table 7-6 – SAW Occupancy per direction

SAW-Occ-per dir*vol by dir*occ		Optimal								
Timing	1	2	3	4	5	6	7	8	9	10
Scramble No [0]/Yes [1]:	0	0	0	0	0	0	0	0	0	0
Cycle length:	60	60	70	70	80	80	90	90	100	100
Effective green EB/WB:	26	29	31	39	36	49	41	59	46	69
Effective green NB/SB:	26	23	31	23	36	23	41	23	46	23
Walk indication for peds (no scramble) EW:	13	16	18	26	23	36	28	46	33	56
FDW for peds (no scramble) EW:	13									
Walk indication for peds (no scramble) NS:	7	4	12	4	17	4	22	4	27	4
FDW for peds (no scramble) NS:	19									
Total delay										
Car	8400	7062	9348	6226	10313	5697	11287	5349	12268	5122
Bus	9740	10371	10898	12947	12069	15788	13250	18801	14437	21947
Bike	387	322	437	276	486	242	536	215	586	194
Ped	28200	27404	29180	27469	30301	28021	31516	28898	32797	30002
Intersection (avg)	17.67	17.08	18.86	17.75	20.11	18.82	21.40	20.15	22.73	21.66

		Criteria		more important ?	Scale
i	j	A	B	A or B	(1-9)
1	2	Car	Bus	B	3
1	3		Bike	B	2
1	4		Ped	B	2
1	5				
1	6				
1	7				
1	8				
2	3	Bus	Bike	A	2
2	4		Ped	A	2
2	5				
2	6				
2	7				
2	8				
3	4	Bike	Ped	B	1
3	5				
3	6				
3	7				
3	8				

Figure 7-1 – Priority rankings between modes

Matrix		Car	Bus	Bike	Ped	normalized principal Eigenvector
Car	1	1	1/3	1/2	1/2	12.23%
Bus	2	3	1	2	2	42.36%
Bike	3	2	1/2	1	1	22.70%
Ped	4	2	1/2	1	1	22.70%

Figure 7-2 –AHP results for priority rankings

Table 7-7 – SAW Priority per mode

SAW-Priority-per mode*vol by dir*occ				Optimal						
Timing	1	2	3	4	5	6	7	8	9	10
Scramble No [0]/Yes [1]:	0	0	0	0	0	0	0	0	0	0
Cycle length:	60	60	70	70	80	80	90	90	100	100
Effective green EB/WB:	26	29	31	39	36	49	41	59	46	69
Effective green NB/SB:	26	23	31	23	36	23	41	23	46	23
Walk indication for peds (no scramble) EW:	13	16	18	26	23	36	28	46	33	56
FDW for peds (no scramble) EW:	13									
Walk indication for peds (no scramble) NS:	7	4	12	4	17	4	22	4	27	4
FDW for peds (no scramble) NS:	19									
Total delay										
Car	10100	8778	11248	8238	12415	8056	13593	8086	14779	8260
Bus	45405	39462	50564	37035	55809	36214	61106	36349	66437	37132
Bike	879	731	991	628	1104	550	1217	489	1331	441
Ped	64014	62208	66238	62354	68783	63607	71541	65598	74448	68105
Intersection (avg)	15.78	14.57	16.92	14.19	18.10	14.21	19.33	14.49	20.58	14.94

Table 7-8 – SAW Priority per direction

SAW-Priority-per dir*vol by dir*occ		Optimal								
Timing	1	2	3	4	5	6	7	8	9	10
Scramble No [0]/Yes [1]:	0	0	0	0	0	0	0	0	0	0
Cycle length:	60	60	70	70	80	80	90	90	100	100
Effective green EB/WB:	26	29	31	39	36	49	41	59	46	69
Effective green NB/SB:	26	23	31	23	36	23	41	23	46	23
Walk indication for peds (no scramble) EW:	13	16	18	26	23	36	28	46	33	56
FDW for peds (no scramble) EW:	13									
Walk indication for peds (no scramble) NS:	7	4	12	4	17	4	22	4	27	4
FDW for peds (no scramble) NS:	19									
Total delay										
Car	10248	8616	11405	7596	12581	6950	13770	6526	14967	6248
Bus	41299	43972	46205	54897	51174	66942	56181	79715	61213	93054
Bike	879	731	991	628	1104	550	1217	489	1331	441
Ped	64014	62208	66238	62354	68783	63607	71541	65598	74448	68105
Intersection (avg)	15.89	15.77	17.04	17.13	18.24	18.84	19.48	20.79	20.74	22.91

Table 7-9 – Delay inputs for AHP & TOPSIS

Timing	1	2	3	4	5	6	7	8	9	10
Scramble No [0]/Yes [1]:	0	0	0	0	0	0	0	0	0	0
Cycle length:	60	60	70	70	80	80	90	90	100	100
Effective green EB/WB:	26	29	31	39	36	49	41	59	46	69
Effective green NB/SB:	26	23	31	23	36	23	41	23	46	23
AHP, TOPSIS Unit, Occ, Pri delay (per mode delay)										
Car	11.64	10.12	12.96	9.49	14.31	9.28	15.66	9.32	17.03	9.52
Bus	23.28	20.23	25.92	18.99	28.61	18.57	31.33	18.64	34.06	19.04
Bike	9.68	8.05	10.92	6.91	12.16	6.05	13.41	5.39	14.65	4.85
Ped	23.11	22.46	23.92	22.52	24.84	22.97	25.83	23.69	26.88	24.59
Intersection	18.89	17.91	19.88	17.71	20.95	17.91	22.08	18.36	23.24	18.99
AHP, TOPSIS Unit, Occ, Pri delay (per dir delay)										
Car	11.81	9.93	13.14	8.75	14.50	8.01	15.87	7.52	17.25	7.20
Bus	10.59	11.27	11.85	14.07	13.12	17.16	14.40	20.44	15.69	23.86
Bike	9.68	8.05	10.92	6.91	12.16	6.05	13.41	5.39	14.65	4.85
Ped	23.11	22.46	23.92	22.52	24.84	22.97	25.83	23.69	26.88	24.59
Intersection (avg)	18.89	17.91	19.88	17.71	20.95	17.91	22.08	18.36	23.24	18.99

Table 7-10 – Inputs for mode weighting for AHP & TOPSIS

Unit: volumes	
Car	569
Bus	92
Bike	40
Ped	1216
Occupancy: vol*occ	
Car	711
Bus (no x2)	460
Bike	40
Ped	1216
Priority: vol*priority*occ	
Car	868
Bus (no x2)	1950
Bike	91
Ped	2760

		Criteria		more important ?	Scale
i	j	A	B	A or B	(1-9)
1	2	Car	Bus	A	6
1	3		Bike	A	9
1	4		Ped	B	2
1	5				
1	6				
1	7				
1	8				
2	3	Bus	Bike	A	2
2	4		Ped	B	9
2	5				
2	6				
2	7				
2	8				
3	4	Bike	Ped	B	9
3	5				
3	6				
3	7				
3	8				

Figure 7-3 – Unit-based rankings between modes

Matrix		Car	Bus	Bike	Ped	normalized principal Eigenvector
Car	1	1	6	9	1/2	34.49%
Bus	2	1/6	1	2	1/9	6.65%
Bike	3	1/9	1/2	1	1/9	4.30%
Ped	4	2	9	9	1	54.56%

Figure 7-4 – AHP results for unit-based rankings

		Criteria		more important ?	Scale
i	j	A	B	A or B	(1-9)
1	2	Car	Bus	A	2
1	3		Bike	A	9
1	4		Ped	B	2
1	5				
1	6				
1	7				
1	8				
2	3	Bus	Bike	A	9
2	4		Ped	B	3
2	5				
2	6				
2	7				
2	8				
3	4	Bike	Ped	B	9
3	5				
3	6				
3	7				
3	8				

Figure 7-5 – Occupancy-based rankings between modes

Matrix		Car	Bus	Bike	Ped	normalized principal Eigenvector
Car	1	1	2	9	1/2	29.73%
Bus	2	1/2	1	9	1/3	19.53%
Bike	3	1/9	1/9	1	1/9	3.41%
Ped	4	2	3	9	1	47.33%

Figure 7-6 – AHP results for occupancy-based rankings

		Criteria		more important ?	Scale
i	j	A	B	A or B	(1-9)
1	2	Car	Bus	B	2
1	3		Bike	A	9
1	4		Ped	B	3
1	5				
1	6				
1	7				
1	8				
2	3	Bus	Bike	A	9
2	4		Ped	B	2
2	5				
2	6				
2	7				
2	8				
3	4	Bike	Ped	B	9
3	5				
3	6				
3	7				
3	8				

Figure 7-7 – Priority-based rankings between modes

Matrix		Car	Bus	Bike	Ped	**normalized principal Eigenvector**
Car	1	1	1/2	9	1/3	19.53%
Bus	2	2	1	9	1/2	29.73%
Bike	3	1/9	1/9	1	1/9	3.41%
Ped	4	3	2	9	1	47.33%

Figure 7-8 – AHP results for priority-based rankings

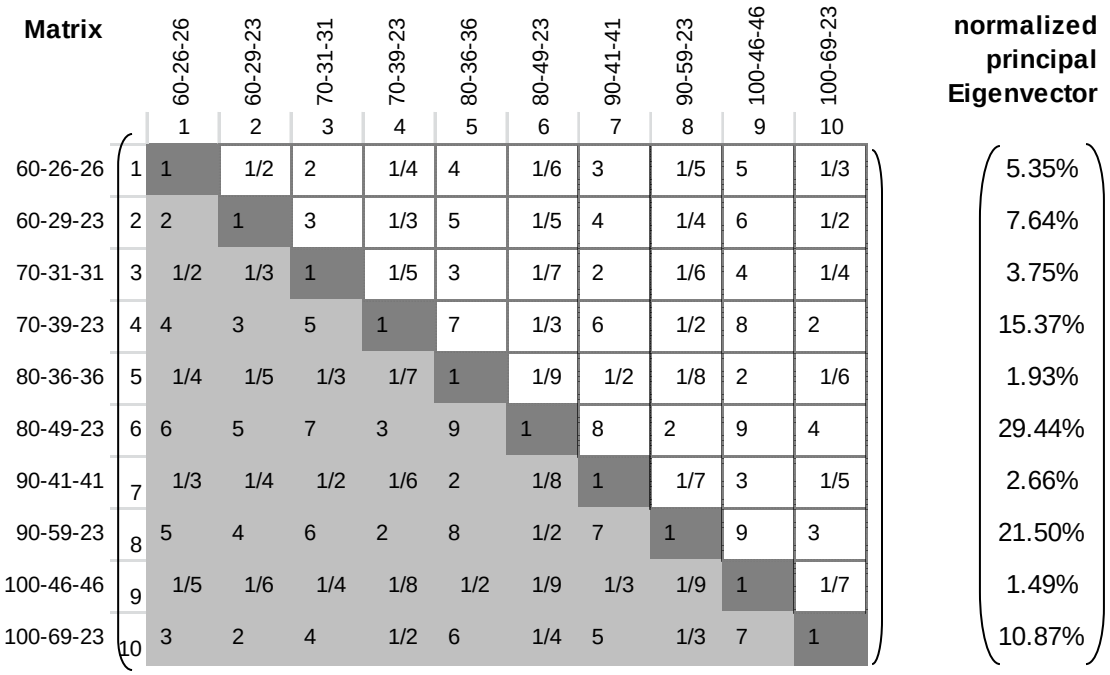

Matrix		60-26-26	60-29-23	70-31-31	70-39-23	80-36-36	80-49-23	90-41-41	90-59-23	100-46-46	100-69-23	normalized principal Eigenvector
		1	2	3	4	5	6	7	8	9	10	
60-26-26	1	1	1/2	2	1/4	4	1/6	3	1/5	5	1/3	5.35%
60-29-23	2	2	1	3	1/3	5	1/5	4	1/4	6	1/2	7.64%
70-31-31	3	1/2	1/3	1	1/5	3	1/7	2	1/6	4	1/4	3.75%
70-39-23	4	4	3	5	1	7	1/3	6	1/2	8	2	15.37%
80-36-36	5	1/4	1/5	1/3	1/7	1	1/9	1/2	1/8	2	1/6	1.93%
80-49-23	6	6	5	7	3	9	1	8	2	9	4	29.44%
90-41-41	7	1/3	1/4	1/2	1/6	2	1/8	1	1/7	3	1/5	2.66%
90-59-23	8	5	4	6	2	8	1/2	7	1	9	3	21.50%
100-46-46	9	1/5	1/6	1/4	1/8	1/2	1/9	1/3	1/9	1	1/7	1.49%
100-69-23	10	3	2	4	1/2	6	1/4	5	1/3	7	1	10.87%

Figure 7-9 – AHP results for per mode delay rankings for car

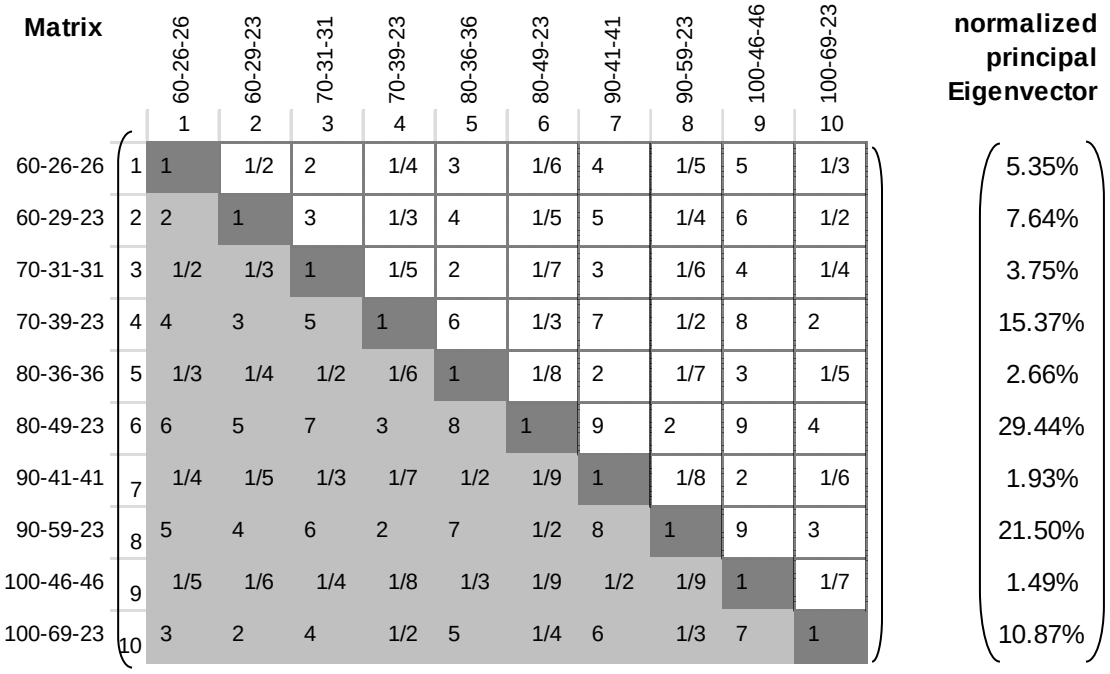

Matrix		60-26-26	60-29-23	70-31-31	70-39-23	80-36-36	80-49-23	90-41-41	90-59-23	100-46-46	100-69-23	normalized principal Eigenvector
		1	2	3	4	5	6	7	8	9	10	
60-26-26	1	1	1/2	2	1/4	3	1/6	4	1/5	5	1/3	5.35%
60-29-23	2	2	1	3	1/3	4	1/5	5	1/4	6	1/2	7.64%
70-31-31	3	1/2	1/3	1	1/5	2	1/7	3	1/6	4	1/4	3.75%
70-39-23	4	4	3	5	1	6	1/3	7	1/2	8	2	15.37%
80-36-36	5	1/3	1/4	1/2	1/6	1	1/8	2	1/7	3	1/5	2.66%
80-49-23	6	6	5	7	3	8	1	9	2	9	4	29.44%
90-41-41	7	1/4	1/5	1/3	1/7	1/2	1/9	1	1/8	2	1/6	1.93%
90-59-23	8	5	4	6	2	7	1/2	8	1	9	3	21.50%
100-46-46	9	1/5	1/6	1/4	1/8	1/3	1/9	1/2	1/9	1	1/7	1.49%
100-69-23	10	3	2	4	1/2	5	1/4	6	1/3	7	1	10.87%

Figure 7-10 – AHP results for per mode delay rankings for bus

Matrix		60-26-26	60-29-23	70-31-31	70-39-23	80-36-36	80-49-23	90-41-41	90-59-23	100-46-46	100-69-23	normalized principal Eigenvector
		1	2	3	4	5	6	7	8	9	10	
60-26-26	1	1	1/2	2	1/3	3	1/4	4	1/5	5	1/6	5.35%
60-29-23	2	2	1	3	1/2	4	1/3	5	1/4	6	1/5	7.64%
70-31-31	3	1/2	1/3	1	1/4	2	1/5	3	1/6	4	1/7	3.75%
70-39-23	4	3	2	4	1	5	1/2	6	1/3	7	1/4	10.87%
80-36-36	5	1/3	1/4	1/2	1/5	1	1/6	2	1/7	3	1/8	2.66%
80-49-23	6	4	3	5	2	6	1	7	1/2	8	1/3	15.37%
90-41-41	7	1/4	1/5	1/3	1/6	1/2	1/7	1	1/8	2	1/9	1.93%
90-59-23	8	5	4	6	3	7	2	8	1	9	1/2	21.50%
100-46-46	9	1/5	1/6	1/4	1/7	1/3	1/8	1/2	1/9	1	1/9	1.49%
100-69-23	10	6	5	7	4	8	3	9	2	9	1	29.44%

Figure 7-11 – AHP results for per mode delay rankings for bike

Matrix		60-26-26	60-29-23	70-31-31	70-39-23	80-36-36	80-49-23	90-41-41	90-59-23	100-46-46	100-69-23	normalized principal Eigenvector
		1	2	3	4	5	6	7	8	9	10	
60-26-26	1	1	1/4	3	1/3	5	1/2	6	2	7	4	10.87%
60-29-23	2	4	1	6	2	8	3	9	5	9	7	29.44%
70-31-31	3	1/3	1/6	1	1/5	3	1/4	4	1/2	5	2	5.35%
70-39-23	4	3	1/2	5	1	7	2	8	4	9	6	21.50%
80-36-36	5	1/5	1/8	1/3	1/7	1	1/6	2	1/4	3	1/2	2.66%
80-49-23	6	2	1/3	4	1/2	6	1	7	3	8	5	15.37%
90-41-41	7	1/6	1/9	1/4	1/8	1/2	1/7	1	1/5	2	1/3	1.93%
90-59-23	8	1/2	1/5	2	1/4	4	1/3	5	1	6	3	7.64%
100-46-46	9	1/7	1/9	1/5	1/9	1/3	1/8	1/2	1/6	1	1/4	1.49%
100-69-23	10	1/4	1/7	1/2	1/6	2	1/5	3	1/3	4	1	3.75%

Figure 7-12 – AHP results for per mode delay rankings for ped

			Criteria											
			Car	Bus	Bike	Ped			Criteria Ranking				Overall Weights	Policies
Policies	1	[	0.0535	0.0535	0.0535	0.1087	]						0.084	60-26-26
	2		0.0764	0.0764	0.0764	0.2944							0.195	60-29-23
	3		0.0375	0.0375	0.0375	0.0535							0.046	70-31-31
	4		0.1537	0.1537	0.1087	0.2150		[	0.3449	]	Car		0.185	70-39-23
	5		0.0193	0.0266	0.0266	0.0266		*	0.0665		Bus	=	0.024	80-36-36
	6		0.2944	0.2944	0.1537	0.1537			0.0430		Bike		0.212	80-49-23
	7		0.0266	0.0193	0.0193	0.0193			0.5456		Ped		0.022	90-41-41
	8		0.2150	0.2150	0.2150	0.0764							0.139	90-59-23
	9		0.0149	0.0149	0.0149	0.0149							0.015	100-46-46
	10	]	0.1087	0.1087	0.2944	0.0375	]						0.078	100-69-23

Figure 7-13 – AHP end result for per mode delays for unit-based

			Criteria											
			Car	Bus	Bike	Ped			Criteria Ranking				Overall Weights	Policies
Policies	1	[	0.0535	0.0535	0.0535	0.1087	]						0.080	60-26-26
	2		0.0764	0.0764	0.0764	0.2944							0.180	60-29-23
	3		0.0375	0.0375	0.0375	0.0535							0.045	70-31-31
	4		0.1537	0.1537	0.1087	0.2150		[	0.2973	]	Car		0.181	70-39-23
	5		0.0193	0.0266	0.0266	0.0266		*	0.1953		Bus	=	0.024	80-36-36
	6		0.2944	0.2944	0.1537	0.1537			0.0341		Bike		0.223	80-49-23
	7		0.0266	0.0193	0.0193	0.0193			0.4733		Ped		0.021	90-41-41
	8		0.2150	0.2150	0.2150	0.0764							0.149	90-59-23
	9		0.0149	0.0149	0.0149	0.0149							0.015	100-46-46
	10	]	0.1087	0.1087	0.2944	0.0375	]						0.081	100-69-23

Figure 7-14 – AHP end result for per mode delays for occupancy-based

			Criteria											
			Car	Bus	Bike	Ped			Criteria Ranking				Overall Weights	Policies
Policies	1	[	0.0535	0.0535	0.0535	0.1087	]						0.080	60-26-26
	2		0.0764	0.0764	0.0764	0.2944							0.179	60-29-23
	3		0.0375	0.0375	0.0375	0.0535							0.045	70-31-31
	4		0.1537	0.1537	0.1087	0.2150		[	0.1950	]	Car		0.181	70-39-23
	5		0.0193	0.0266	0.0266	0.0266		*	0.2970		Bus	=	0.025	80-36-36
	6		0.2944	0.2944	0.1537	0.1537			0.0340		Bike		0.223	80-49-23
	7		0.0266	0.0193	0.0193	0.0193			0.4730		Ped		0.021	90-41-41
	8		0.2150	0.2150	0.2150	0.0764							0.149	90-59-23
	9		0.0149	0.0149	0.0149	0.0149							0.015	100-46-46
	10	]	0.1087	0.1087	0.2944	0.0375	]						0.081	100-69-23

Figure 7-15 – AHP end result for per mode delays for priority-based

Matrix		60-26-26	60-29-23	70-31-31	70-39-23	80-36-36	80-49-23	90-41-41	90-59-23	100-46-46	100-69-23	normalized principal Eigenvector
		1	2	3	4	5	6	7	8	9	10	
60-26-26	1	1	1/2	2	1/3	3	1/4	4	1/5	5	1/6	5.35%
60-29-23	2	2	1	3	1/2	4	1/3	5	1/4	6	1/5	7.64%
70-31-31	3	1/2	1/3	1	1/4	2	1/5	3	1/6	4	1/7	3.75%
70-39-23	4	3	2	4	1	5	1/2	6	1/3	7	1/4	10.87%
80-36-36	5	1/3	1/4	1/2	1/5	1	1/6	2	1/7	3	1/8	2.66%
80-49-23	6	4	3	5	2	6	1	7	1/2	8	1/3	15.37%
90-41-41	7	1/4	1/5	1/3	1/6	1/2	1/7	1	1/8	2	1/9	1.93%
90-59-23	8	5	4	6	3	7	2	8	1	9	1/2	21.50%
100-46-46	9	1/5	1/6	1/4	1/7	1/3	1/8	1/2	1/9	1	1/9	1.49%
100-69-23	10	6	5	7	4	8	3	9	2	9	1	29.44%

Figure 7-16 – AHP results for per direction delay rankings for car

Matrix		60-26-26	60-29-23	70-31-31	70-39-23	80-36-36	80-49-23	90-41-41	90-59-23	100-46-46	100-69-23	normalized principal Eigenvector
		1	2	3	4	5	6	7	8	9	10	
60-26-26	1	1	2	3	5	4	8	6	9	7	9	29.44%
60-29-23	2	1/2	1	2	4	3	7	5	8	6	9	21.50%
70-31-31	3	1/3	1/2	1	3	2	6	4	7	5	8	15.37%
70-39-23	4	1/5	1/4	1/3	1	1/2	4	2	5	3	6	7.64%
80-36-36	5	1/4	1/3	1/2	2	1	5	3	6	4	7	10.87%
80-49-23	6	1/8	1/7	1/6	1/4	1/5	1	1/3	2	1/2	3	2.66%
90-41-41	7	1/6	1/5	1/4	1/2	1/3	3	1	4	2	5	5.35%
90-59-23	8	1/9	1/8	1/7	1/5	1/6	1/2	1/4	1	1/3	2	1.93%
100-46-46	9	1/7	1/6	1/5	1/3	1/4	2	1/2	3	1	4	3.75%
100-69-23	10	1/9	1/9	1/8	1/6	1/7	1/3	1/5	1/2	1/4	1	1.49%

Figure 7-17 – AHP results for per direction delay rankings for bus

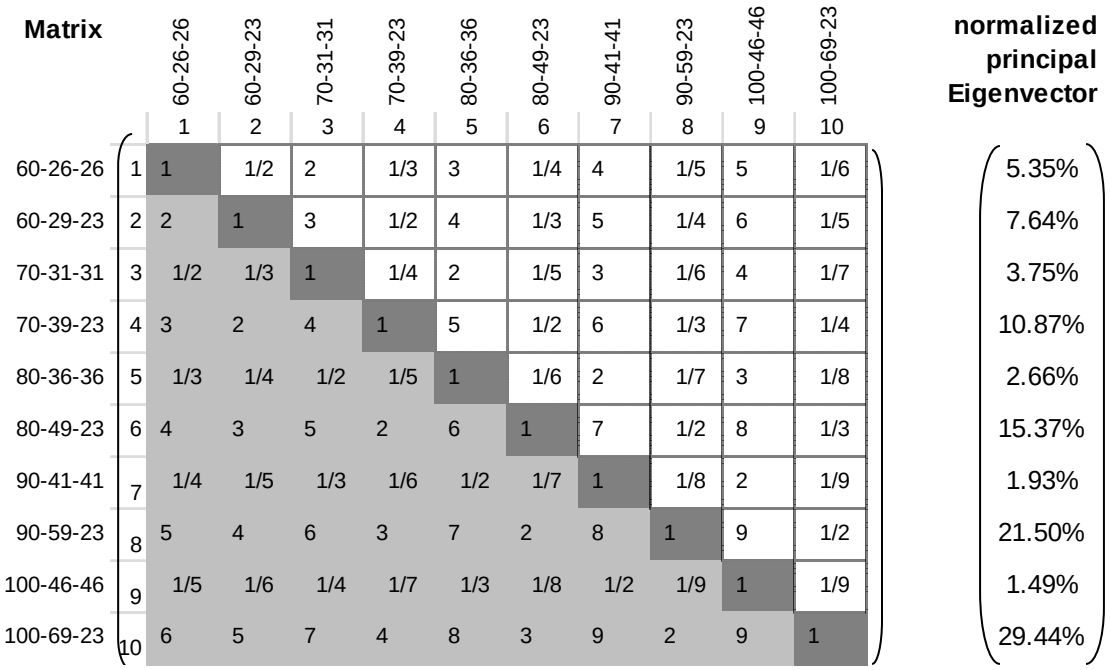

Matrix		60-26-26	60-29-23	70-31-31	70-39-23	80-36-36	80-49-23	90-41-41	90-59-23	100-46-46	100-69-23	normalized principal Eigenvector
		1	2	3	4	5	6	7	8	9	10	
60-26-26	1	1	1/2	2	1/3	3	1/4	4	1/5	5	1/6	5.35%
60-29-23	2	2	1	3	1/2	4	1/3	5	1/4	6	1/5	7.64%
70-31-31	3	1/2	1/3	1	1/4	2	1/5	3	1/6	4	1/7	3.75%
70-39-23	4	3	2	4	1	5	1/2	6	1/3	7	1/4	10.87%
80-36-36	5	1/3	1/4	1/2	1/5	1	1/6	2	1/7	3	1/8	2.66%
80-49-23	6	4	3	5	2	6	1	7	1/2	8	1/3	15.37%
90-41-41	7	1/4	1/5	1/3	1/6	1/2	1/7	1	1/8	2	1/9	1.93%
90-59-23	8	5	4	6	3	7	2	8	1	9	1/2	21.50%
100-46-46	9	1/5	1/6	1/4	1/7	1/3	1/8	1/2	1/9	1	1/9	1.49%
100-69-23	10	6	5	7	4	8	3	9	2	9	1	29.44%

Figure 7-18 – AHP results for per direction delay rankings for bike

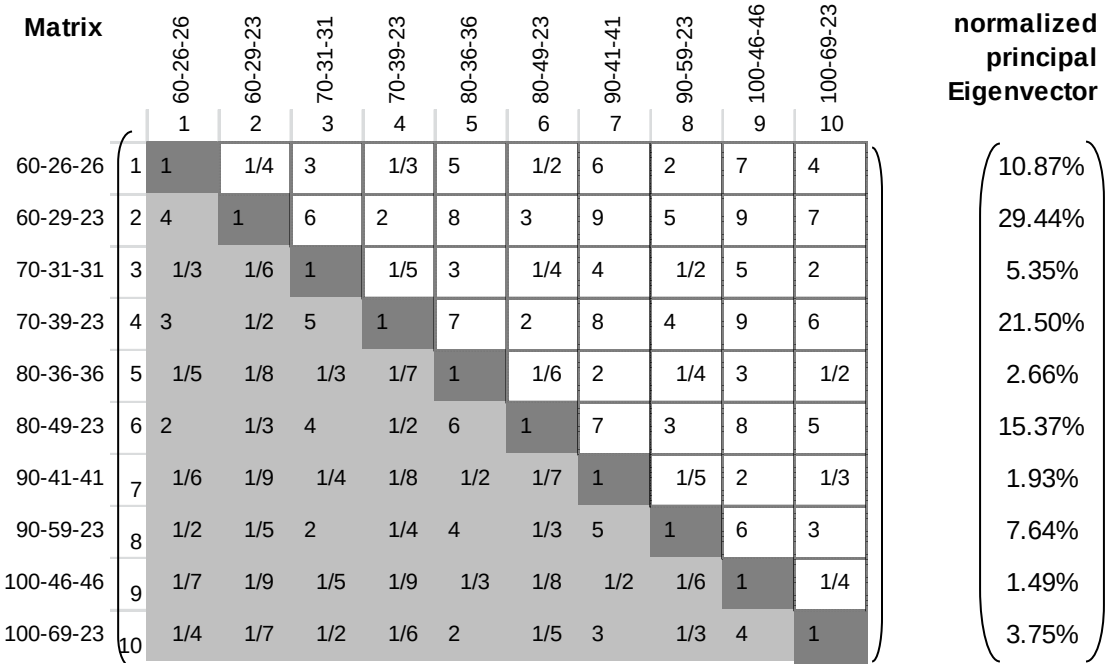

Matrix		60-26-26	60-29-23	70-31-31	70-39-23	80-36-36	80-49-23	90-41-41	90-59-23	100-46-46	100-69-23	normalized principal Eigenvector
		1	2	3	4	5	6	7	8	9	10	
60-26-26	1	1	1/4	3	1/3	5	1/2	6	2	7	4	10.87%
60-29-23	2	4	1	6	2	8	3	9	5	9	7	29.44%
70-31-31	3	1/3	1/6	1	1/5	3	1/4	4	1/2	5	2	5.35%
70-39-23	4	3	1/2	5	1	7	2	8	4	9	6	21.50%
80-36-36	5	1/5	1/8	1/3	1/7	1	1/6	2	1/4	3	1/2	2.66%
80-49-23	6	2	1/3	4	1/2	6	1	7	3	8	5	15.37%
90-41-41	7	1/6	1/9	1/4	1/8	1/2	1/7	1	1/5	2	1/3	1.93%
90-59-23	8	1/2	1/5	2	1/4	4	1/3	5	1	6	3	7.64%
100-46-46	9	1/7	1/9	1/5	1/9	1/3	1/8	1/2	1/6	1	1/4	1.49%
100-69-23	10	1/4	1/7	1/2	1/6	2	1/5	3	1/3	4	1	3.75%

Figure 7-19 – AHP results for per mode delay rankings for ped

			Criteria												
			Car	Bus	Bike	Ped				Criteria Ranking				Overall Weights	Policies
Policies	1	[	0.0535	0.2944	0.0535	0.1087	]							0.100	60-26-26
	2		0.0764	0.2150	0.0764	0.2944								0.205	60-29-23
	3		0.0375	0.1537	0.0375	0.0535								0.054	70-31-31
	4		0.1087	0.0764	0.1087	0.2150			[	0.3449	]		Car	0.165	70-39-23
	5		0.0266	0.1087	0.0266	0.0266		*		0.0665			Bus	= 0.032	80-36-36
	6		0.1537	0.0266	0.1537	0.1537				0.0430			Bike	0.145	80-49-23
	7		0.0193	0.0535	0.0193	0.0193				0.5456			Ped	0.022	90-41-41
	8		0.2150	0.0193	0.2150	0.0764			]					0.126	90-59-23
	9		0.0149	0.0375	0.0149	0.0149								0.016	100-46-46
	10	]	0.2944	0.0149	0.2944	0.0375								0.136	100-69-23

Figure 7-20 – AHP end result for per direction delays for unit-based

			Criteria												
			Car	Bus	Bike	Ped				Criteria Ranking				Overall Weights	Policies
Policies	1	[	0.0535	0.2944	0.0535	0.1087	]							0.127	60-26-26
	2		0.0764	0.2150	0.0764	0.2944								0.207	60-29-23
	3		0.0375	0.1537	0.0375	0.0535								0.068	70-31-31
	4		0.1087	0.0764	0.1087	0.2150			[	0.2973	]		Car	0.153	70-39-23
	5		0.0266	0.1087	0.0266	0.0266		*		0.1953			Bus	= 0.043	80-36-36
	6		0.1537	0.0266	0.1537	0.1537				0.0341			Bike	0.129	80-49-23
	7		0.0193	0.0535	0.0193	0.0193				0.4733			Ped	0.026	90-41-41
	8		0.2150	0.0193	0.2150	0.0764			]					0.111	90-59-23
	9		0.0149	0.0375	0.0149	0.0149								0.019	100-46-46
	10	]	0.2944	0.0149	0.2944	0.0375								0.118	100-69-23

Figure 7-21 – AHP end result for per direction delays for occupancy-based

			Criteria												
			Car	Bus	Bike	Ped				Criteria Ranking				Overall Weights	Policies
Policies	1	[	0.0535	0.2944	0.0535	0.1087	]							0.151	60-26-26
	2		0.0764	0.2150	0.0764	0.2944								0.221	60-29-23
	3		0.0375	0.1537	0.0375	0.0535								0.080	70-31-31
	4		0.1087	0.0764	0.1087	0.2150			[	0.1950	]		Car	0.149	70-39-23
	5		0.0266	0.1087	0.0266	0.0266		*		0.2970			Bus	= 0.051	80-36-36
	6		0.1537	0.0266	0.1537	0.1537				0.0340			Bike	0.116	80-49-23
	7		0.0193	0.0535	0.0193	0.0193				0.4730			Ped	0.029	90-41-41
	8		0.2150	0.0193	0.2150	0.0764			]					0.091	90-59-23
	9		0.0149	0.0375	0.0149	0.0149								0.022	100-46-46
	10	]	0.2944	0.0149	0.2944	0.0375								0.090	100-69-23

Figure 7-22 – AHP end result for per direction delays for priority-based

				Options:									
				1	2	3	4	5	6	7	8	9	10
			Importance	60-26-26	60-29-23	70-31-31	SAW TOPSIS 70-39-23	80-36-36	AHP 80-49-23	90-41-41	90-59-23	100-46-46	100-69-23
Criteria:	1	Car	0.346	11.6398	10.1164	12.9624	9.49424	14.307	9.28366	15.6649	9.3184	17.0317	9.51895
	2	Bus	0.066	23.2796	20.2329	25.9249	18.9885	28.6139	18.5673	31.3298	18.6368	34.0634	19.0379
	3	Bike	0.043	9.68174	8.05386	10.9189	6.91088	12.1608	6.05368	13.4059	5.38699	14.6533	4.85366
	4	Ped	0.546	23.1148	22.4626	23.918	22.5154	24.8368	22.9678	25.8327	23.6867	26.8825	24.592
			Score	**0.71**	**0.89**	**0.54**	**0.96**	**0.37**	**0.95**	**0.19**	**0.89**	**0.00**	**0.82**

Figure 7-23 – TOPSIS results with SAW & AHP optimals for Unit-based, per mode

				Options:									
				1	2	3	4	5	6	7	8	9	10
			Importance	60-26-26	AHP 60-29-23	70-31-31	SAW 70-39-23	80-36-36	TOPSIS 80-49-23	90-41-41	90-59-23	100-46-46	100-69-23
Criteria:	1	Car	0.346	11.81	9.92954	13.1431	8.75388	14.4991	8.01	15.8691	7.52091	17.2483	7.20099
	2	Bus	0.066	10.5873	11.2724	11.8451	14.0732	13.1188	17.161	14.4024	20.4355	15.6923	23.855
	3	Bike	0.043	9.68174	8.05386	10.9189	6.91088	12.1608	6.05368	13.4059	5.38699	14.6533	4.85366
	4	Ped	0.546	23.1148	22.4626	23.918	22.5154	24.8368	22.9678	25.8327	23.6867	26.8825	24.592
			Score	**0.58**	**0.75**	**0.45**	**0.85**	**0.32**	**0.88**	**0.19**	**0.85**	**0.10**	**0.80**

Figure 7-24 – TOPSIS results with SAW & AHP optimals for Unit-based, per direction

				Options:									
				1	2	3	4	5	6	7	8	9	10
			Importance	60-26-26	60-29-23	70-31-31	SAW TOPSIS 70-39-23	80-36-36	AHP 80-49-23	90-41-41	90-59-23	100-46-46	100-69-23
Criteria:	1	Car	0.297	11.6398	10.1164	12.9624	9.49424	14.307	9.28366	15.6649	9.3184	17.0317	9.51895
	2	Bus	0.195	23.2796	20.2329	25.9249	18.9885	28.6139	18.5673	31.3298	18.6368	34.0634	19.0379
	3	Bike	0.034	9.68174	8.05386	10.9189	6.91088	12.1608	6.05368	13.4059	5.38699	14.6533	4.85366
	4	Ped	0.473	23.1148	22.4626	23.918	22.5154	24.8368	22.9678	25.8327	23.6867	26.8825	24.592
			Score	**0.708**	**0.892**	**0.540**	**0.961**	**0.365**	**0.957**	**0.184**	**0.907**	**0.000**	**0.842**

Figure 7-25 – TOPSIS results with SAW & AHP optimals for Occupancy-based, per mode

				Options:									
				1	2	3	4	5	6	7	8	9	10
			Importance	60-26-26	SAW AHP 60-29-23	70-31-31	TOPSIS 70-39-23	80-36-36	80-49-23	90-41-41	90-59-23	100-46-46	100-69-23
Criteria:	1	Car	0.297	11.81	9.92954	13.1431	8.75388	14.4991	8.01	15.8691	7.52091	17.2483	7.20099
	2	Bus	0.195	10.5873	11.2724	11.8451	14.0732	13.1188	17.161	14.4024	20.4355	15.6923	23.855
	3	Bike	0.034	9.68174	8.05386	10.9189	6.91088	12.1608	6.05368	13.4059	5.38699	14.6533	4.85366
	4	Ped	0.473	23.1148	22.4626	23.918	22.5154	24.8368	22.9678	25.8327	23.6867	26.8825	24.592
			Score	**0.66**	**0.79**	**0.55**	**0.82**	**0.45**	**0.75**	**0.35**	**0.67**	**0.27**	**0.60**

Figure 7-26 – TOPSIS results with SAW & AHP optimals for Occupancy-based, per direction

				Options:									
				1	2	3	4	5	6	7	8	9	10
			Importance	60-26-26	60-29-23	70-31-31	SAW TOPSIS 70-39-23	80-36-36	AHP 80-49-23	90-41-41	90-59-23	100-46-46	100-69-23
Criteria:	1	Car	0.195	11.6398	10.1164	12.9624	9.49424	14.307	9.28366	15.6649	9.3184	17.0317	9.51895
	2	Bus	0.297	23.2796	20.2329	25.9249	18.9885	28.6139	18.5673	31.3298	18.6368	34.0634	19.0379
	3	Bike	0.034	9.68174	8.05386	10.9189	6.91088	12.1608	6.05368	13.4059	5.38699	14.6533	4.85366
	4	Ped	0.473	23.1148	22.4626	23.918	22.5154	24.8368	22.9678	25.8327	23.6867	26.8825	24.592
			Score	**0.708**	**0.892**	**0.540**	**0.962**	**0.365**	**0.957**	**0.184**	**0.907**	**0.000**	**0.842**

Figure 7-27 – TOPSIS results with SAW & AHP optimals for Priority-based, per mode

				Options:									
				1	2	3	4	5	6	7	8	9	10
			Importance	60-26-26	SAW AHP TOPSIS 60-29-23	70-31-31	70-39-23	80-36-36	80-49-23	90-41-41	90-59-23	100-46-46	100-69-23
Criteria:	1	Car	0.195	11.81	9.92954	13.1431	8.75388	14.4991	8.01	15.8691	7.52091	17.2483	7.20099
	2	Bus	0.297	10.5873	11.2724	11.8451	14.0732	13.1188	17.161	14.4024	20.4355	15.6923	23.855
	3	Bike	0.034	9.68174	8.05386	10.9189	6.91088	12.1608	6.05368	13.4059	5.38699	14.6533	4.85366
	4	Ped	0.473	23.1148	22.4626	23.918	22.5154	24.8368	22.9678	25.8327	23.6867	26.8825	24.592
			Score	**0.78**	**0.85**	**0.70**	**0.78**	**0.60**	**0.63**	**0.51**	**0.50**	**0.42**	**0.41**

Figure 7-28 – TOPSIS results with SAW & AHP optimals for Priority-based, per direction

7.2 Reinforcement Learning Agent

A series of experiments were analyzed using the reinforcement learning agent described in the previous chapter. The same case study used for the MADM methods was also constructed in VISSIM and tested with the RL agent, thus similar geometry and demands by mode were analyzed.

For each scenario, the focus of the analysis was centered on the evolution of the agent's knowledge and the improvements in the signal performance over time. Also, the analysis covers the actual signal timing settings found during the training period and how the control decisions changed over time.

The agent was allowed to make a new decision every 2 seconds and to operate the signal without a maximum green time, but with a minimum green time equal to the crossing time for each of the pedestrian crossings. Therefore, once a phase was selected it was maintained for 18 seconds for the E-W direction and for 24 seconds for the N-S direction. The states were scaled down by a factor of 1/2, thus for example 2 additional vehicles would be perceived by the agent as an increase of 1 in the state. On each direction, the states for vehicles and buses together could have a range of values between 0 and 15, for pedestrians between 0 and 5, and for bicycles between 0 and 5.

The relative importance of the modes (w_i in the reward structure) was similar to the factors found in by AHP for the priority rankings, such that the vehicles were weighted by a factor of 1.2, buses by 4.2, and bicycles and pedestrians by 2.3; the values of the factors in the penalty function were the following: $\beta_1 = 1$, $\beta_2 = 12$, $\beta_3 = 0.5$, and $\beta_4 = 0.1$.

Similar to the MADM methods, the observed volumes for each mode were simulated in three conditions: 1) actual demands found in the field, called "Vol x1", 2) double the demands for all modes, called "Vol x2", and 3) triple the demands for all modes, called "Vol x3".

Based on preliminary results, it was estimated that the agents would require about 200 replications to reach a plateau in the performance. Cases with lower volumes are expected to have a faster convergence because the links do not reach higher occupancies and thus the state space visited is smaller. Based on these estimates it was decided to perform 275 replications to increase confidence in the values observed on the plateau. Each replication was run for 15 simulation minutes.

First, the scenario with the original demands (Vol x1) was simulated. Results for the evolution of the duration of the two phases is shown in Figure 7-29 . A few observations can be made from this figure, starting with the little learning that occurred over time. Convergence seemed to occur very quickly within the first replications, with a particular pattern of long and short durations of the E-W phase and a steady short duration of the N-S phase.

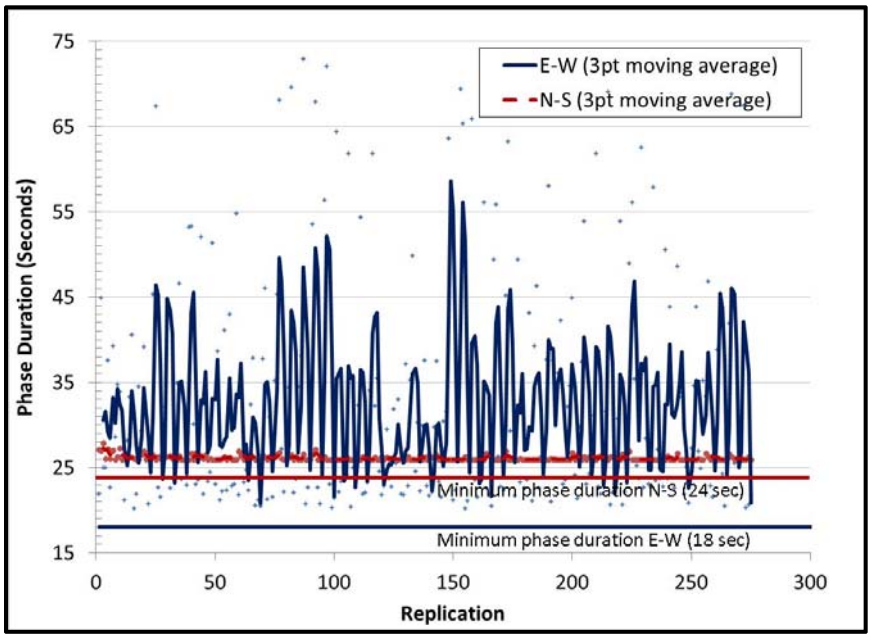

Figure 7-29 – Agent training – Average Phase duration for field demands (Vol x1)

The distribution of the demands by direction is about 89% of the vehicular traffic on the E-W direction and the remaining 11% in the N-S direction, whereas pedestrian traffic is about 75% in the E-W direction compared to 25% in the N-S direction. Therefore, traffic is heavily sided to the E-W direction and it is expected to receive additional green time.

The pattern observed for the N-S direction in Figure 7-29 is steady and on par with the minimum green time, suggesting that demands are constantly lower than this threshold and the minimum duration was enough to process the arriving traffic. However, the pattern observed for E-W shows simulation runs with long green times followed by replications with low green times. This indicates that such low traffic volume may result in arrival patterns with significant variations, which were in turn replicated by the traffic signal behavior. Recall that the vehicular volume per approach in the E-W direction is only 275 vehicles (for each direction on average), which is roughly 40% the capacity of an approach assuming it can process 700 vph in ideal conditions and without left turns.

In terms of the measures of performance, Figure 7-30 shows the average delay and number of stops for all modes combined. Variations in the average delay and stops are significantly lower than those seen for the green times, confirming that the system responded to the traffic arrival patterns trying to maintain the quality of service. Also, there was no strong correlation between replications with shorter green times and lower delays or fewer number of stops, which supports this claim.

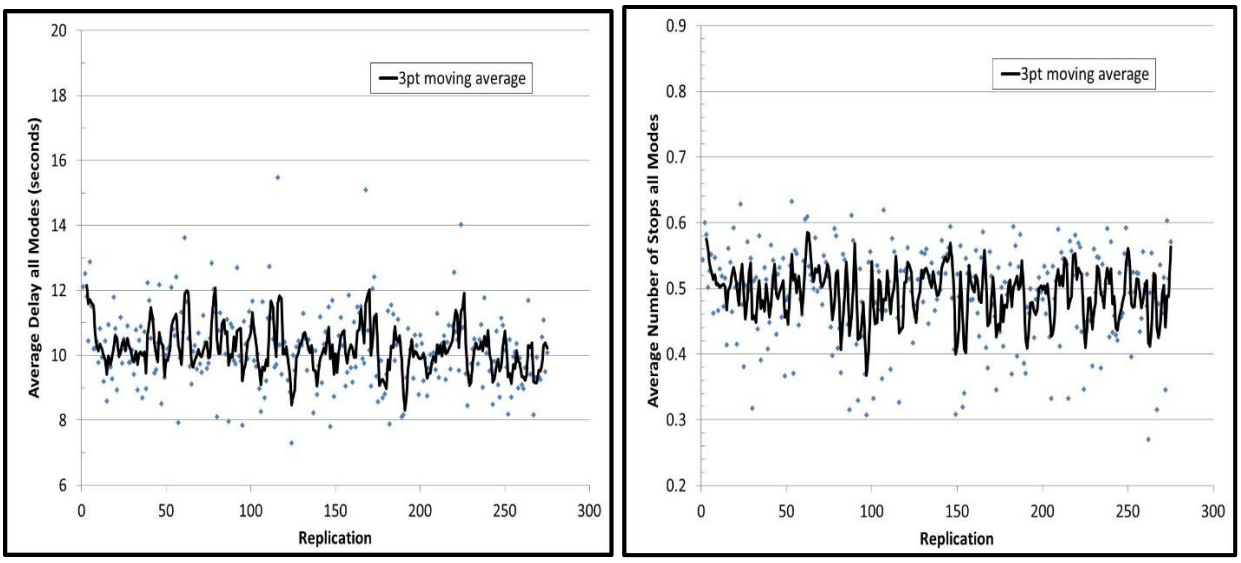

a) Average delay for all modes b) Average number of stops for all modes

Figure 7-30 – Agent training – Average delay and number of stops for all modes (Vol x1)

Further analysis showed that the average delays were very similar for all modes. Results based on the last 30 replications showed that average delay for vehicles was 10.1 s, for buses 10.5 s, for pedestrians 9.3 s, and for bicyclists 10.6 s. In addition their standard variation for a given mode increased as their volume was lower. For example, the standard variation for bicycles was 6.7 whereas for vehicles it was 2.0. This is expected since modes with low volumes will not have a significant contribution in the demands and therefore the signal will not necessarily provide the right of way based on their arrivals, but on modes with greater volume.

Overall, results from the agent showed fast convergence and generated very wide range of green times in the E-W direction, generating delays that were similar for all transportation modes and thus providing an equitable service.

The second case for demands that double the original volumes (Vol x2) is described next. It is noted that demands from all modes are multiplied by 2, keeping the demand ratios by direction and modes constant.

With higher traffic, the number of states visited increased and the learning process lasted for an increased number of replications, reaching a plateau around the 50th replication. Similar figures were generated for this scenario compared to Vol x1, with the evolution of the phase duration shown in Figure 7-31. The duration of the N-S phase remained at the bare minimum, terminating the phase right after the threshold of 24 seconds was reached. This is similar to the case with the original demand levels since the volumes on N-S are very low to justify 24 seconds of green, imposed due to pedestrian clearance requirements. On the other hand, the E-W direction showed significant variations between replications, but with a lower magnitude than those observed in the previous case with lower demands. Greater volumes reduce the effects of random arrivals in the operation of the signals, and thus the reduction in the green time variations was expected.

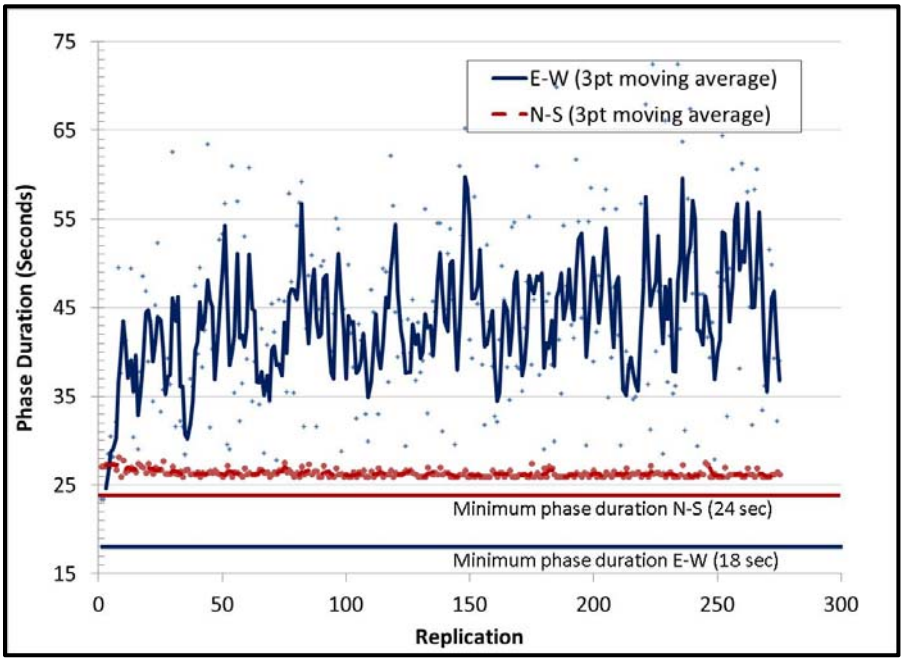

Figure 7-31 – Agent training – Average phase duration for double the field demand (Vol x2)

The learning process in terms of performance can be observed in the evolution of the average delay and number of stops, as shown in Figure 7-32. Delays and number of stops decreased over time, reaching levels that were higher than in the previous case, but similar in magnitude. The scale of the figures for this case is the same as those with the original volumes from the field, thus they are directly comparable.

Regarding the delay distribution by mode, in the last 30 replications the average delays were 11.7 s for vehicles, 12.6 for buses, 10.1 for pedestrians, and 14.2 for bicycles. Similarly, the standard deviation of the delay for bicycles and buses were the greatest, 5.61 and 4.70 respectively, compared to automobiles (1.59) and pedestrians (0.97).

Overall, this scenario showed a somewhat signal behavior given the higher volumes, and the performance of the modes was balanced and with small increases in the delays compared to the previous case. The learning behavior of the agents was more notorious and can be appreciated during a greater number of replications.

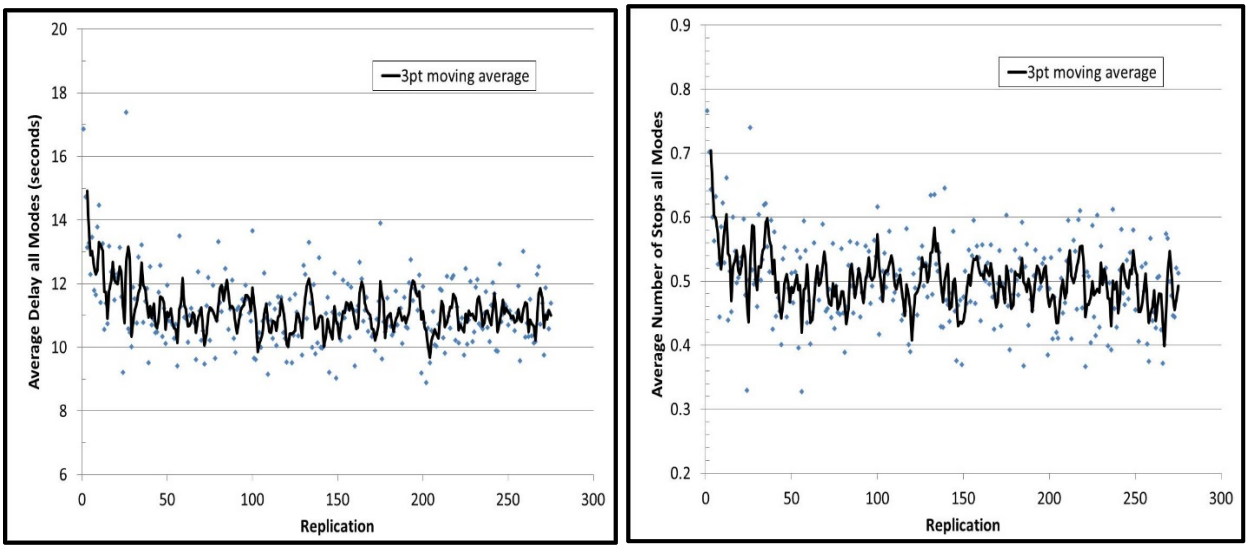

a) Average delay for all modes b) Average number of stops for all modes

Figure 7-32 – Agent training – Average delay and number of stops for all modes (Vol x2)

Lastly, the scenario with three times the demands found in the field was analyzed (vol x3). For this scenario, links on the E-W direction had longer queues and the allocated number of potential states in this direction (a total of 15 states with a scale factor of 1/2) was quickly filled in the E-W when the green indication was given to the N-S direction. Therefore, it was decided to scale down all modes by a factor of 1/3, instead of a factor of 1/2 used for the previous cases. This allowed the agent to observe changes in the state when up to 45 vehicles were sensed in the E-W direction, instead of only 30 vehicles. Given that scale change was applied to all modes, comparisons to previous cases are still valid. Another alternative to modify the agent for higher volumes was to increase the range of values for the E-W space, but this will void fair comparisons with the previous cases.

Results for the duration of the green times in the two phases during the training period are shown in Figure 7-33. Significant variation was found in the average green times in the E-W direction, contrasted with a steady low value for the N-S direction. This trend is similar to the Vol x2 case, but the average green times in the E-W direction for the Vol x3 case in last 30 replications was 53 seconds (ranging between 35 and 71 seconds) compared 46 seconds in the Vol x2 case (ranging between 28 to 64 seconds). Thus, as expected, cycles lengths increased in the Vol x3 case compared to the Vol x2 case.

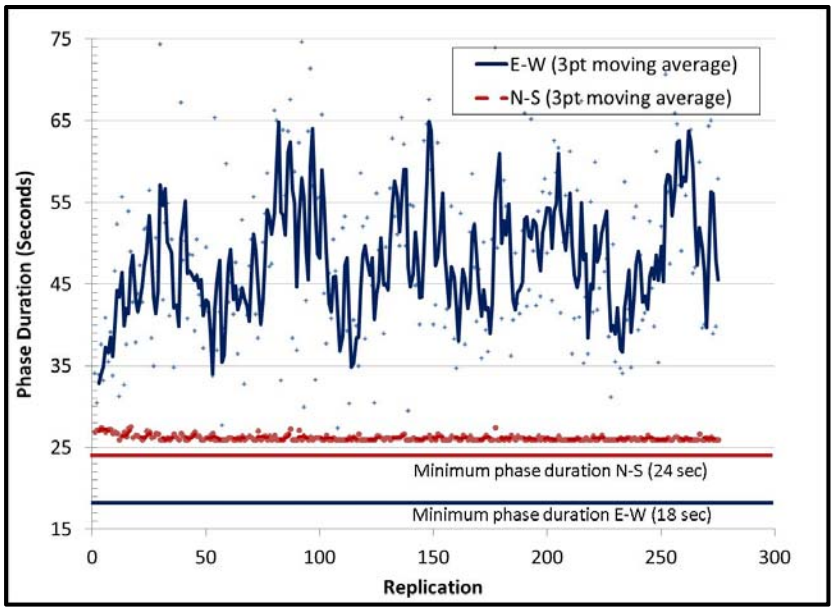

Figure 7-33 – Agent training – Average phase duration for triple the field demand (Vol x3)

In terms of the average delay and number of stops, some improvement was achieved throughout the replications to reach combined levels that were higher than in the previous case (Vol x2), as seen in Figure 7-34. This was expected given the higher demands and longer queues. A closer observation of the delays per mode showed that they increased proportionally with exception of the pedestrian delays. Based on the last 30 replications, vehicles experienced on average 16.5 seconds of delay, buses 16.8 seconds, pedestrians 10.1 seconds, and bicycles 16.2 seconds.

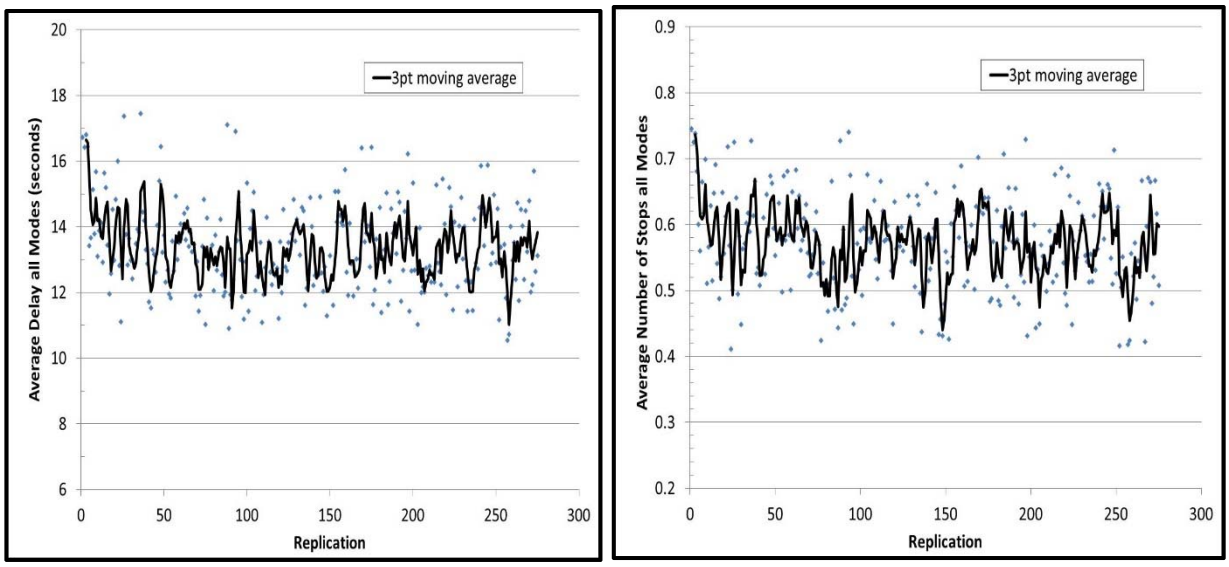

a) Average delay for all modes b) Average number of stops for all modes

Figure 7-34 – Agent training – Average delay and number of stops for all modes (Vol x3)

8 ADDITIONAL WORK

Additional work involving sensitivity analysis of signal timing was carried out as an extension of the project. The work involved running the aforementioned analytical program to determine the occasions at which an intersection operating with a scramble phase is preferred to one without. This expands upon the work carried out by Yang and Benekohal (2011), where genetic algorithms were used to determine the optimal intersection operation mode (with or without a scramble phase), by including varying cycle lengths and a new pedestrian delay formula. A hypothetical standard intersection was simulated with one exclusive left, through, and right-turn lane in each of four approaches all with the same vehicular and pedestrian volume for each approach. Three runs were performed for different through volumes: 200, 700, and 1200 vehicles per hour. Right-turning traffic varied from 200 to 1200 vehicles per hour with intervals of 250. Pedestrian demand varied from 400 to 2000 pedestrians in each parallel crossing with intervals of 400. When a scramble crossing was applied, the pedestrian demand from each corner was split evenly between the two parallel crosswalks and the diagonal.

In addition, left turns remained the same throughout all iterations at 100 left turns per approach to reduce excessive cycle lengths as a result of protected left turn phases. To provide adequate service time for these vehicles, the length of these phases were determined by giving two seconds for each left-turner arriving per cycle, with an additional three seconds for startup lost time. Three seconds of change and clearance were present after each phase. All other signal timing characteristics were similar to the previous implementation.

The following charts illustrate this analysis, where the optimal cycle length and operation mode corresponds with the lowest intersection delay for all modes. A practitioner would in theory

first find the optimal cycle length for the given volumes, and then use the next chart to find the walk time. Figure 8-1, Figure 8-3, and Figure 8-5 show the optimal cycle length that is chosen for a respective demand. Figure 8-2, Figure 8-4, and Figure 8-6 show whether the optimal operation is with or without a scramble, and if it is with a scramble, then the duration of that length. In the walk time charts, the dark blue (0 seconds of walk time) represents no scramble.

A couple of trends are very noticeable from these charts: As the through volume increases, the minimum cycle length for the lowest right-turn and pedestrian volumes goes from 70 seconds to 120 seconds to 160 seconds; and as the right-turn volume increases, the optimal cycle length also increases due to the greater volume and conflicts with pedestrians. There appears to be less of a clear trend as pedestrian volume increases, possibly indicating that for this volume condition, increasing pedestrians do not affect delays as much as increasing vehicular volumes does. However, based on the no scramble/scramble mode and walk time charts, it is noted that increased pedestrians are accounted for in the increased length of the scramble phase. For example, there is a gradual change from no scramble and a scramble phase with 6 seconds of walk to as much as a scramble phase with 16 seconds of walk. Increasing pedestrian volume but keeping right-turning volume constant increases the length of the scramble but the cycle length is generally kept the same to prevent additional delay to all users. A possible explanation on why the scramble length remains mostly constant when right-turning vehicles increase is that the pedestrians remain the same, so there is no need to extend the walk indication for pedestrians (although there is a need to increase cycle length).

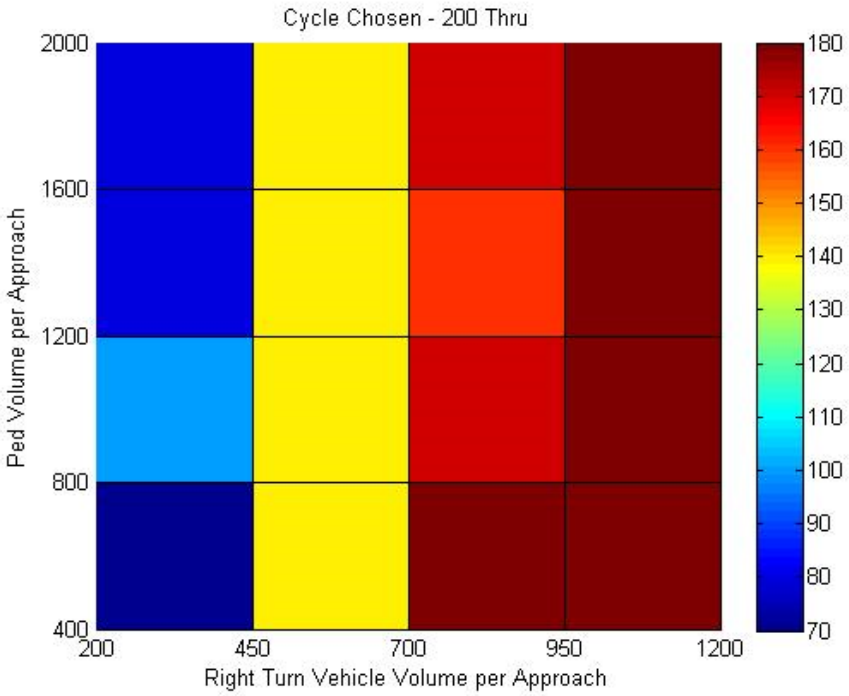

Figure 8-1 – Optimal cycle length for 200 Thru

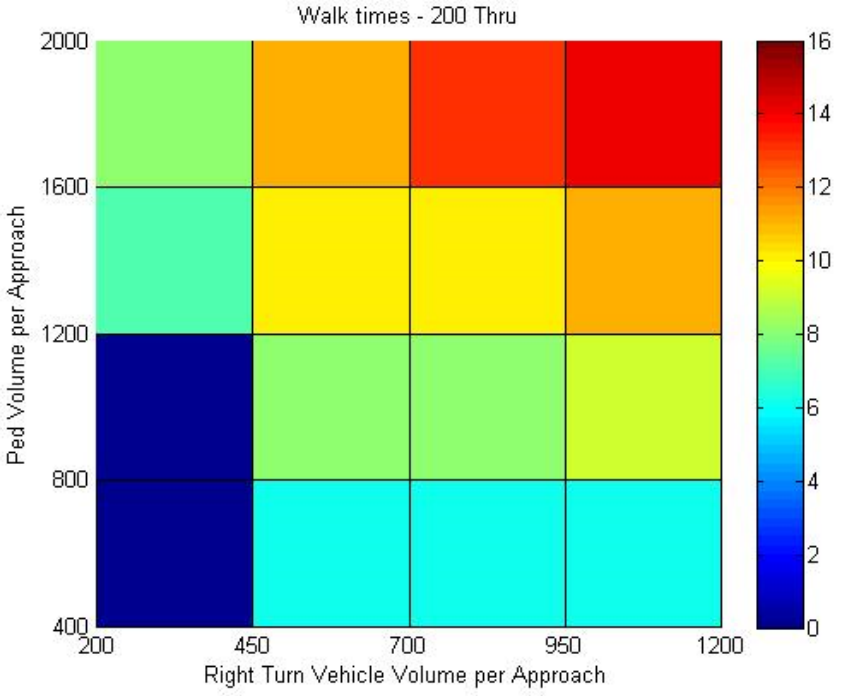

Figure 8-2 – Optimal operation mode and walk time for 200 Thru

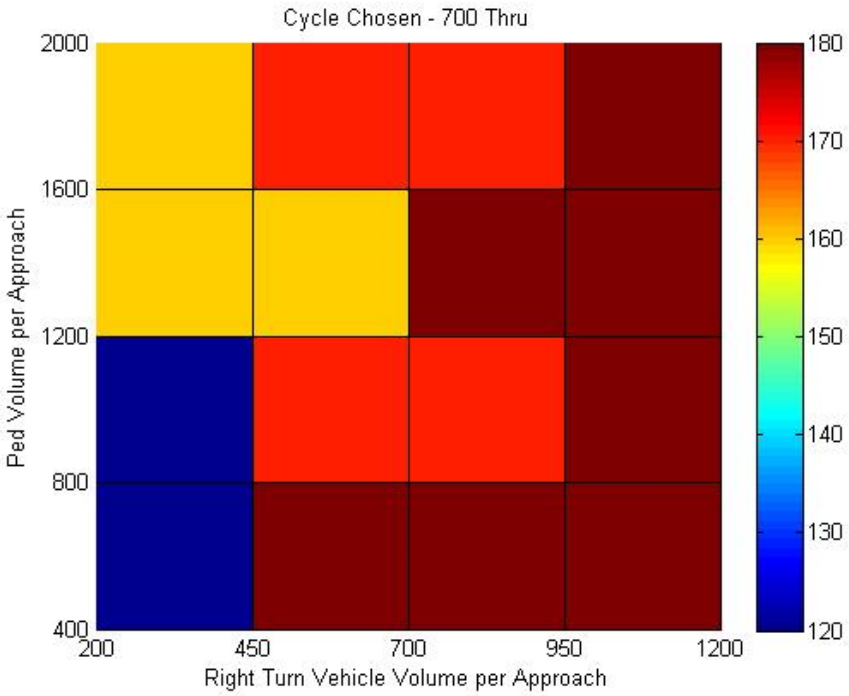

Figure 8-3 – Optimal cycle length for 700 Thru

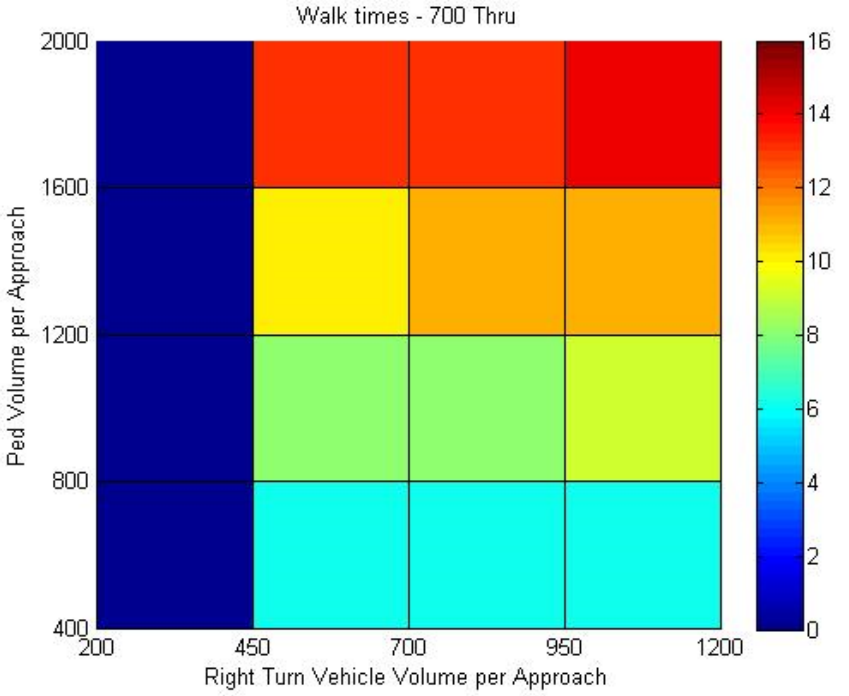

Figure 8-4 – Optimal operation mode and walk time for 700 Thru

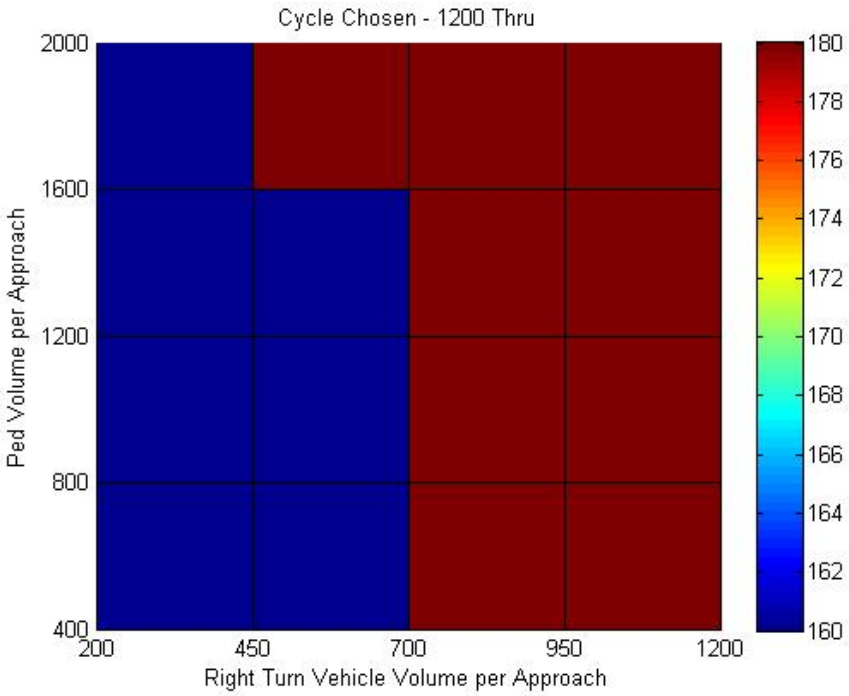

Figure 8-5 – Optimal cycle length for 1200 Thru

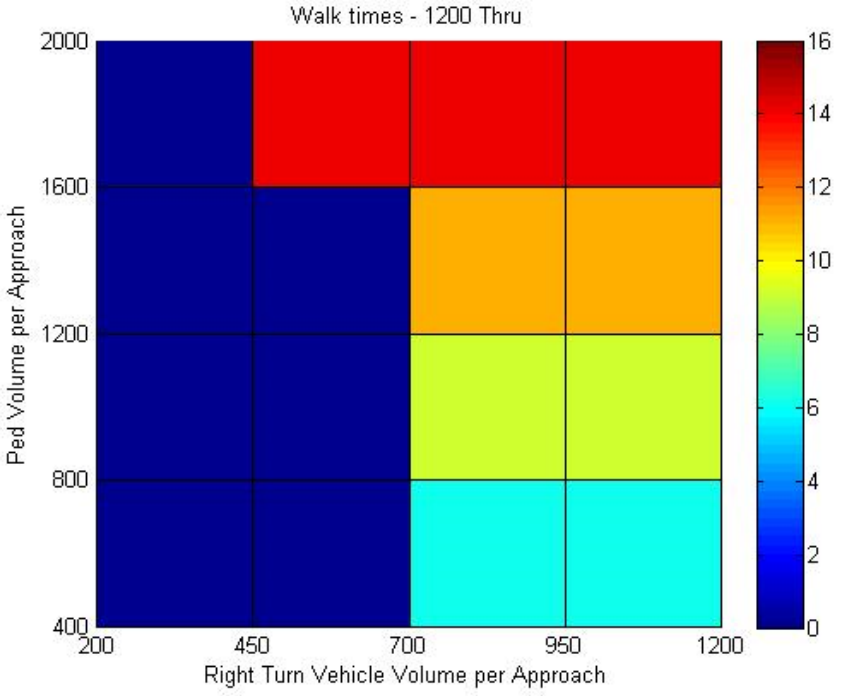

Figure 8-6 – Optimal operation mode and walk time for 1200 Thru

9 CONCLUSIONS

Results indicate that all three analytical MADM methods (SAW, AHP, and TOPSIS) selected signal timing settings that followed general expectations in terms of cycle length and green time splits; however, their optimal alternatives were not always the same. The sensitivity of the solutions also varied across strategies, with SAW and TOPSIS being more sensitive than AHP.

SAW and TOPSIS are well-suited for optimal selection of multi-modal signal timing parameters because they can deal with multiple criteria (modes of transportation and their characteristics) and large number of alternatives with simplicity. In TOPSIS, the utility of each mode is assumed to linearly increase or decrease across the range of alternatives, thus special consideration should be given to non-linear functions. While SAW considers each alternative separately, TOPSIS uses all alternatives together to normalize their utility, therefore a more careful and comprehensive selection of alternatives is required.

AHP allows inputs based on qualitative and quantitative comparisons between alternatives or modes, but it requires an extensive number of pairwise comparisons for problems with large number of alternatives. Matrix manipulations may also be an issue if many alternatives are considered at a given time. However, the method is less subject to variation when the reliability of the input data is questionable and when the alternatives are not evenly distributed across the utility range.

The results from this study support the potential application of the MADM methods as an alternative to more traditional approaches; however, further research is recommended to

extend them for multimodal traffic control. Also, the sensitivity charts provided in Chapter 8 illustrate the cases in which a scramble pedestrian phase is beneficial for all modes combined. However, additional analysis of multiple configurations and scenarios are needed to develop strong guidelines that are practice-ready.

In terms of the agent-based strategy to control the signals, results showed that the agent effectively balanced delays for all modes and was sensitive to changes in the demands. Average delays and number of stops per mode obtained with the agent-based approach confirmed that the green time variations responded to variability in the demand, since the delays were relatively stable for all replications once a performance plateau was reached. Overall, the agent-based approach showed potential for multi-modal applications and it is appealing since it reacts in real time to changes in the traffic conditions of all modes.

Further studies on parameter selection and alternative algorithms are needed to strengthen the resources available to researchers and practitioners, and to generate stronger guidelines on how to use these types of cycle-free and adaptive strategies in a real world intersection. Additional research is also recommended to include a multimodal analysis along a corridor and in networks with closely-spaced intersections, where coordination of green times between adjacent signals is important.

10 REFERENCES

1. Abdulhai, B., Pringle, R., and Karakoulas, G.J. Reinforcement Learning for True Adaptive Traffic Signal Control, ASCE Journal of Transportation Engineering, Vol. 129, No 3, (2003): 278-285.
2. Alecsandru, C, Rouhieh, B., Huang, K. C. "Multimodal Signal Optimization of Urban Arterials and Bicycle Paths: Case Study." TRB Annual Meeting, 2010.
3. Appl, M., and Brauer, W. Fuzzy Model-Based Reinforcement Learning. Presented at the European Symposium on Intelligent Techniques, Germany. 2000
4. Bakker, B., Steingrover, M., Schouten, R., Nijhuis, and E., Kester, L. Cooperative Multi-agent Reinforcement Learning of Traffic Lights. Gama, J., Camacho, R., Brazdil, P.B., Jorge, A.M., Torgo, L. (eds.) ECML 2005. LNCS (LNAI), Vol. 3720. Springer, Heidelberg. 2005
5. Bhattacharya, P. and Virkler, M. R. "Optimization for Pedestrian and Vehicular Delay in a Signal Network." *Transportation Research Record* 1939 (2005): 115-122.
6. Bingham, E. Neurofuzzy Traffic Signal Control. Master's thesis, Dept. of Engineering Physics and Mathematics, Helsinki Univ. of Technology, Helsinki, Finland. 1998
7. Bingham, E. Reinforcement Learning in Neurofuzzy Traffic Signal Control, European Journal of Operations Research, Vol. 131, No. 2, (2001): 232–241.
8. Camponogara, E., and Kraus, W. Jr. Distributed Learning Agents in Urban Traffic Control. Progress in Artificial Intelligence: Proceedings of the 11th Portuguese Conference on Artificial Intelligence (EPIA). 2003
9. Carsten, O. M. J., Sherborne, D. J. and Rothengatter, J. A. "Intelligent Traffic Signals for Pedestrians: Evaluation of Trials in Three Countries." *Transportation Research Part C*, Vol. 6, (1998): 213-229.

10. Christofa, E., Skabardonis, A. “Traffic Signal Optimization with Application of Transit Signal Priority to an Isolated Intersection.” *Transportation Research Record* 2259 (2011): 192-201.
11. Choy, M. C., Cheu, R. L., Srinivasan, D., and Logi, F. Real-time Coordinated Signal Control Using Agents with Online Reinforcement Learning. Proceedings of the 82nd Transportation Research Board Annual Meeting. Washington, D.C. 2003
12. De Oliveira, D., Bazzan, A. L.C., Castro da Silva, B., Basso, E.W., and Nunez, L. Reinforcement Learning based Control of Traffic Lights in Non-stationary Environments: A Case Study in a Microscopic Simulator. Fourth European Workshop on Multi-Agent Systems. Portugal. 2006
13. Dion, F., Hesham R., and Kang, Y-S. "Comparison of Delay Estimates at Under-saturated and Over-saturated Pre-timed Signalized Intersections." *Transportation Research Part B: Methodological* 38.2 (2004): 99-122.
14. El-Tantawy, S. and Abdulhai, B. “An Agent-based Learning Towards Decentralized and Coordinated Traffic Signal Control”. 13th International IEEE Annual Conference on Intelligent Transportation Systems. Portugal, 2010.
15. “Highway Capacity Manual 2010.” *Transportation Research Board.* 5th Ed.
16. Ishaque, M. M. and Noland, R. B. “Multimodal Microsimulation of Vehicle and Pedestrian Signal Timings.” *Transportation Research Record* 1939 (2005): 107-114.
17. Goepel, Klaus. *AHPcalc*. Computer software. *BPMSG*. Vers. 31.05.13. 8 May 2013.
18. HCS 2010. Computer software. McTrans.
19. “Manual on Uniform Traffic Control Devices.” *U.S. Department of Transportation: Federal Highway Administration*. 2009 Ed revision 2.
20. Mateo, J.R. S.C. *Multi-Criteria Analysis in the Renewable Energy Industry*, Green Energy and Technology, DOI: 10.1007/978-1-4471-2346-0_7, Springer-Verlag London Limited 2012
21. Medina, J.C., Benekohal, R.F. Q-learning and Approximate Dynamic Programming for Traffic Control: Case Study for an Oversaturated Network. Presented at the 91st Annual Meeting of the Transportation Research Board. Washington, D.C. 2012.

22. Medina, J.C., Hajbabaie, A., Benekohal, R.F. Effects of Metered Entry Volume on an Oversaturated Network with Dynamic Signal Timing. Transportation Research Record, Vol. 2356, (2013): 53-60.

    Noland, R. "Pedestrian Travel Times and Motor Vehicle Traffic Signals." *Transportation Research Record* 1553.1 (1996): 28-33.
23. Richter, S., Aberdeen, D., and Yu, J. Natural Actor-Critic for Road Traffic Optimisation. Advances in Neural Information Processing Systems MIT Press, Cambridge, MA, (2007):1169-1176.
24. Rouhieh, B. “Multi-Modal Traffic Signal Design under Safety and Operations Constraints.” Master Thesis. Corcordia University. 2008.
25. Shladover, S. E., Kim, Z., Cao, M., Sharafsaleh, A. and Li, J-Q. “Bicyclist Intersection Crossing Times: Quantitative Measurements for Selecting Signal Timing.” *Transportation Research Record* 2128 (2009): 86-95.
26. Taylor, D. and Mahmassani, H. “Coordinating traffic signals for Bicycle Progression.” *Transportation Research Record* 1705 (2010): 85-92.
27. Thorpe, T. Vehicle Traffic Light Control Using SARSA, Master Thesis, Department of Computer Science, Colorado State University. 1997
28. Triantaphyllou, E., B. Shu, Sanchez, S. N., and Ray, T. "Multi-Criteria Decision Making: An Operations Research Approach." *Encyclopedia of Electrical and Electronics Engineering*. Vol. 15. New York, NY: John Wiley & Sons, 1998. 175-86.
29. *Triptych*. Computer software. Vers. 4. Statistical Design Institute.
30. Virkler, M. "Signal Coordination Benefits for Pedestrians." *Transportation Research Record* 1636 (1998): 77-82.
31. Watkins, C.J.C.H. Learning from Delayed Rewards. PhD Thesis, King’s College, Cambridge, England. 1989
32. Watkins, C.J.C.H. and Dayan, P. Technical note: Q-learning. Machine Learning, Vol. 8, (1992): 279-292.
33. Wiering, M. Multi-Agent Reinforcement Learning for Traffic Light Control. Proceedings 17th International Conference on Machine Learning, (2000): 1151–1158.

34. Xie, Y. Development and Evaluation of an Arterial Adaptive Traffic Signal Control System using Reinforcement Learning, Doctoral Dissertation, Texas A&M University: College Station, TX. 2007
35. Yang, Z. and Benekohal, R. "Use of Genetic Algorithm for Phase Optimization at Intersections with Minimization of Vehicle and Pedestrian Delays." Transportation Research Record 2264 (2011): 54-64.
36. Yeh, C-H. "A Problem-based Selection of Multi-attribute Decision-making Methods." *International Transactions in Operational Research* 9.2 (2002): 169-81.
37. Yoon, K. P., & Hwang, C-L. *Multiple Attribute Decision making: An Introduction.* Sage University Paper series on Quantitative Applications in the Social Sciences. 07-104. Thousand Oaks, CA: Sage. 1995
38. Zhang, Y., Xie, Y., and Ye, Y. Development and Evaluation of a Multi-Agent Based Neuro-Fuzzy Arterial Traffic Signal Control System, Texas A&M University, pp. 122 (SWUTC #473700- 00092-1). 2007
39. Zolfani, S. H., and Antucheviciene, J. "Team Member Selecting Based on AHP and TOPSIS Grey." *Engineering Economics* 23.4 (2013): 425-34.

11 Appendix

Table of Contents

11.1 Appendix A – MADM Results for Saturated and Oversaturated Conditions

Table 11-1 – v/c ratios for saturated (volume x3)

Cycle length:	60	60	70	70	80	80	90	90	100	100
Effective green EB/WB:	26	28	31	38	36	48	41	58	46	68
Effective green NB/SB:	26	24	31	24	36	24	41	24	46	24
Walk indication for peds (no scramble) EW:	13	15	18	25	23	35	28	45	33	55
Walk indication for peds (no scramble) NS:	7	5	12	5	17	5	22	5	27	5
X=v/c for EB_T:	0.736	0.683	0.720	0.588	0.709	0.532	0.700	0.495	0.693	0.476
X=v/c for EB_R:	0.143	0.124	0.137	0.096	0.133	0.082	0.130	0.073	0.127	0.069
X=v/c for WB_T:	0.962	0.893	0.941	0.768	0.926	0.695	0.915	0.647	0.906	0.622
X=v/c for WB_R:	1.226	1.067	1.176	0.824	1.141	0.703	1.115	0.631	1.096	0.596
X=v/c for NB_T:	0.091	0.099	0.089	0.115	0.088	0.132	0.087	0.148	0.086	0.158
X=v/c for NB_R:	0.244	0.272	0.237	0.337	0.232	0.412	0.228	0.496	0.226	0.553
X=v/c for SB_T:	0.179	0.193	0.175	0.226	0.172	0.258	0.170	0.290	0.168	0.309

Table 11-2 – v/c ratios for oversaturated (volume x4)

Cycle length:	70	70	80	80	90	90	90	100	100	110
Effective green EB/WB:	31	37	36	47	41	56	57	46	67	76
Effective green NB/SB:	31	25	36	25	41	26	25	46	25	26
Walk indication for peds (no scramble) EW:	18	24	23	34	28	43	44	33	54	63
Walk indication for peds (no scramble) NS:	12	6	17	6	22	7	6	27	6	7
X=v/c for EB_T:	0.960	0.805	0.945	0.724	0.934	0.683	0.671	0.924	0.635	0.616
X=v/c for EB_R:	0.258	0.170	0.247	0.138	0.240	0.124	0.120	0.234	0.109	0.103
X=v/c for WB_T:	1.255	1.051	1.235	0.946	1.220	0.893	0.878	1.208	0.830	0.804
X=v/c for WB_R:	2.219	1.465	2.128	1.187	2.062	1.067	1.034	2.013	0.937	0.890
X=v/c for NB_T:	0.119	0.147	0.117	0.168	0.116	0.182	0.189	0.114	0.211	0.223
X=v/c for NB_R:	0.353	0.493	0.345	0.619	0.339	0.716	0.773	0.334	0.964	1.095
X=v/c for SB_T:	0.233	0.289	0.229	0.330	0.226	0.357	0.371	0.224	0.413	0.436

				Options:									
				1	2	3	4	5	6	7	8	9	10
			Importance	60-26-26	60-28-24	70-31-31	AHP 70-38-24	80-36-36	SAW TOPSIS 80-48-24	90-41-41	90-58-24	100-46-46	100-68-24
Criteria:	1	Car	0.345	43.8038	30.4139	41.5236	18.52	40.7143	15.692	40.74	14.733	41.2803	14.8558
	2	Bus	0.066	87.6076	60.8278	83.0471	37.04	81.4287	31.3841	81.48	29.466	82.5607	29.7116
	3	Bike	0.043	9.78003	8.6743	11.0297	7.45895	12.2843	6.5477	13.542	5.83919	14.802	5.60049
	4	Ped	0.546	23.6231	23.1477	24.4483	23.0976	25.3918	23.4791	26.4142	24.1481	27.4917	25.0219
			Score	**0.22**	**0.51**	**0.20**	**0.87**	**0.17**	**0.96**	**0.12**	**0.93**	**0.08**	**0.88**

Figure 11-1 – TOPSIS results with SAW & AHP optimals for Unit-based, per mode (volume x3)

				Options:									
				1	2	3	4	5	6	7	8	9	10
			Importance	60-26-26	60-28-24	70-31-31	AHP 70-38-24	80-36-36	SAW TOPSIS 80-48-24	90-41-41	90-58-24	100-46-46	100-68-24
Criteria:	1	Car	0.345	45.1079	31.0523	42.7484	18.2125	41.9151	14.6087	41.9449	12.8727	42.5053	12.396
	2	Bus	0.066	35.738	26.4653	33.9484	20.4216	33.2879	22.3923	33.288	26.2389	33.7043	30.0696
	3	Bike	0.043	9.78003	8.6743	11.0297	7.45895	12.2843	6.5477	13.542	5.83919	14.802	5.60049
	4	Ped	0.546	23.6231	23.1477	24.4483	23.0976	25.3918	23.4791	26.4142	24.1481	27.4917	25.0219
			Score	**0.205**	**0.477**	**0.187**	**0.831**	**0.157**	**0.929**	**0.115**	**0.927**	**0.076**	**0.879**

Figure 11-2 – TOPSIS results with SAW & AHP optimals for Unit-based, per direction (volume x3)

				Options:									
				1	2	3	4	5	6	7	8	9	10
			Importance	60-26-26	60-28-24	70-31-31	AHP 70-38-24	80-36-36	TOPSIS 80-48-24	90-41-41	SAW 90-58-24	100-46-46	100-68-24
Criteria:	1	Car	0.297	43.8038	30.4139	41.5236	18.52	40.7143	15.692	40.74	14.733	41.2803	14.8558
	2	Bus	0.195	87.6076	60.8278	83.0471	37.04	81.4287	31.3841	81.48	29.466	82.5607	29.7116
	3	Bike	0.034	9.78003	8.6743	11.0297	7.45895	12.2843	6.5477	13.542	5.83919	14.802	5.60049
	4	Ped	0.473	23.6231	23.1477	24.4483	23.0976	25.3918	23.4791	26.4142	24.1481	27.4917	25.0219
			Score	**0.19**	**0.50**	**0.18**	**0.87**	**0.16**	**0.96**	**0.12**	**0.94**	**0.08**	**0.90**

Figure 11-3 - TOPSIS results with SAW & AHP optimals for Occupancy-based, per mode (volume x3)

				Options:									
				1	2	3	4	5	6	7	8	9	10
			Importance	60-26-26	60-28-24	70-31-31	AHP 70-38-24	80-36-36	SAW TOPSIS 80-48-24	90-41-41	90-58-24	100-46-46	100-68-24
Criteria:	1	Car	0.297	45.1079	31.0523	42.7484	18.2125	41.9151	14.6087	41.9449	12.8727	42.5053	12.396
	2	Bus	0.195	35.738	26.4653	33.9484	20.4216	33.2879	22.3923	33.288	26.2389	33.7043	30.0696
	3	Bike	0.034	9.78003	8.6743	11.0297	7.45895	12.2843	6.5477	13.542	5.83919	14.802	5.60049
	4	Ped	0.473	23.6231	23.1477	24.4483	23.0976	25.3918	23.4791	26.4142	24.1481	27.4917	25.0219
			Score	**0.20**	**0.49**	**0.18**	**0.84**	**0.16**	**0.92**	**0.12**	**0.88**	**0.08**	**0.80**

Figure 11-4 - TOPSIS results with SAW & AHP optimals for Occupancy-based, per mode (volume x3)

				Options:									
				1	2	3	4	5	6	7	8	9	10
			Importance	60-26-26	60-28-24	70-31-31	AHP 70-38-24	80-36-36	TOPSIS 80-48-24	90-41-41	SAW 90-58-24	100-46-46	100-68-24
Criteria:	1	Car	0.195	43.8038	30.4139	41.5236	18.52	40.7143	15.692	40.74	14.733	41.2803	14.8558
	2	Bus	0.297	87.6076	60.8278	83.0471	37.04	81.4287	31.3841	81.48	29.466	82.5607	29.7116
	3	Bike	0.034	9.78003	8.6743	11.0297	7.45895	12.2843	6.5477	13.542	5.83919	14.802	5.60049
	4	Ped	0.473	23.6231	23.1477	24.4483	23.0976	25.3918	23.4791	26.4142	24.1481	27.4917	25.0219
			Score	**0.19**	**0.50**	**0.18**	**0.87**	**0.16**	**0.96**	**0.12**	**0.94**	**0.08**	**0.90**

Figure 11-5 – TOPSIS results with SAW & AHP optimals for Priority-based, per mode (volume x3)

				Options:									
				1	2	3	4	5	6	7	8	9	10
			Importance	60-26-26	60-28-24	70-31-31	SAW AHP 70-38-24	80-36-36	TOPSIS 80-48-24	90-41-41	90-58-24	100-46-46	100-68-24
Criteria:	1	Car	0.195	45.1079	31.0523	42.7484	18.2125	41.9151	14.6087	41.9449	12.8727	42.5053	12.396
	2	Bus	0.297	35.738	26.4653	33.9484	20.4216	33.2879	22.3923	33.288	26.2389	33.7043	30.0696
	3	Bike	0.034	9.78003	8.6743	11.0297	7.45895	12.2843	6.5477	13.542	5.83919	14.802	5.60049
	4	Ped	0.473	23.6231	23.1477	24.4483	23.0976	25.3918	23.4791	26.4142	24.1481	27.4917	25.0219
			Score	**0.24**	**0.55**	**0.22**	**0.87**	**0.19**	**0.91**	**0.14**	**0.78**	**0.10**	**0.67**

Figure 11-6 – TOPSIS results with SAW & AHP optimals for Priority-based, per direction (volume x3)

				Options:									
				1	2	3	4	5	6	7	8	9	10
			Importance	70-31-31	AHP 70-37-25	80-36-36	80-47-25	90-41-41	90-56-26	TOPSIS 90-57-25	100-46-46	SAW 100-67-25	110-76-26
Criteria:	1	Car	0.346	149.04	65.2055	141.624	38.6675	136.824	30.7252	28.6166	133.703	25.4929	25.8359
	2	Bus	0.066	298.08	130.411	283.248	77.3351	273.648	61.4504	57.2331	267.406	50.9858	51.6718
	3	Bike	0.043	11.086	7.97658	12.3469	7.00866	13.6111	6.63231	6.25627	14.8776	5.65475	5.47129
	4	Ped	0.546	24.7245	23.4887	25.681	23.801	26.7171	24.4751	24.4191	27.8091	25.2513	26.2234
			Score	**0.13**	**0.69**	**0.11**	**0.89**	**0.11**	**0.94**	**0.95**	**0.12**	**0.92**	**0.89**

Figure 11-7 – TOPSIS results with SAW & AHP optimals for Unit-based, per mode (volume x4)

				Options:									
				1	2	3	4	5	6	7	8	9	10
			Importance	70-31-31	70-37-25	80-36-36	80-47-25	SAW 90-41-41	90-56-26	TOPSIS 90-57-25	100-46-46	100-67-25	AHP 110-76-26
Criteria:	1	Car	0.346	154.761	66.3939	147.033	37.9387	142.026	28.9561	26.3781	138.764	21.0892	19.5231
	2	Bus	0.066	113.661	57.8553	108.169	43.1752	104.654	41.6663	42.4612	102.399	52.7291	64.8794
	3	Bike	0.043	11.086	7.97658	12.3469	7.00866	13.6111	6.63231	6.25627	14.8776	5.65475	5.47129
	4	Ped	0.546	24.7245	23.4887	25.681	23.801	26.7171	24.4751	24.4191	27.8091	25.2513	26.2234
			Score	**0.12**	**0.66**	**0.11**	**0.87**	**0.10**	**0.92**	**0.94**	**0.12**	**0.92**	**0.89**

Figure 11-8 – TOPSIS results with SAW & AHP optimals for Unit-based, per direction (volume x4)

				Options:									
				1	2	3	4	5	6	7	8	9	10
			Importance	70-31-31	70-37-25	80-36-36	80-47-25	90-41-41	90-56-26	TOPSIS 90-57-25	100-46-46	SAW AHP 100-67-25	110-76-26
Criteria:	1	Car	0.297	149.04	65.2055	141.624	38.6675	136.824	30.7252	28.6166	133.703	25.4929	25.8359
	2	Bus	0.195	298.08	130.411	283.248	77.3351	273.648	61.4504	57.2331	267.406	50.9858	51.6718
	3	Bike	0.034	11.086	7.97658	12.3469	7.00866	13.6111	6.63231	6.25627	14.8776	5.65475	5.47129
	4	Ped	0.473	24.7245	23.4887	25.681	23.801	26.7171	24.4751	24.4191	27.8091	25.2513	26.2234
			Score	**0.11**	**0.69**	**0.10**	**0.89**	**0.11**	**0.94**	**0.96**	**0.12**	**0.93**	**0.90**

Figure 11-9 – TOPSIS results with SAW & AHP optimals for Occupancy-based, per mode (volume x4)

				Options:									
				1	2	3	4	5	6	7	8	9	10
			Importance	70-31-31	70-37-25	80-36-36	80-47-25	90-41-41	90-56-26	TOPSIS 90-57-25	SAW 100-46-46	100-67-25	AHP 110-76-26
Criteria:	1	Car	0.297	154.761	66.3939	147.033	37.9387	142.026	28.9561	26.3781	138.764	21.0892	19.5231
	2	Bus	0.195	113.661	57.8553	108.169	43.1752	104.654	41.6663	42.4612	102.399	52.7291	64.8794
	3	Bike	0.034	11.086	7.97658	12.3469	7.00866	13.6111	6.63231	6.25627	14.8776	5.65475	5.47129
	4	Ped	0.473	24.7245	23.4887	25.681	23.801	26.7171	24.4751	24.4191	27.8091	25.2513	26.2234
			Score	**0.12**	**0.68**	**0.10**	**0.88**	**0.11**	**0.93**	**0.94**	**0.12**	**0.91**	**0.85**

Figure 11-10 – TOPSIS results with SAW & AHP optimals for Occupancy-based, per direction (volume x4)

				Options:									
				1	2	3	4	5	6	7	8	9	10
			Importance	70-31-31	70-37-25	80-36-36	80-47-25	90-41-41	90-56-26	TOPSIS 90-57-25	100-46-46	SAW AHP 100-67-25	110-76-26
Criteria:	1	Car	0.195	149.04	65.2055	141.624	38.6675	136.824	30.7252	28.6166	133.703	25.4929	25.8359
	2	Bus	0.297	298.08	130.411	283.248	77.3351	273.648	61.4504	57.2331	267.406	50.9858	51.6718
	3	Bike	0.034	11.086	7.97658	12.3469	7.00866	13.6111	6.63231	6.25627	14.8776	5.65475	5.47129
	4	Ped	0.473	24.7245	23.4887	25.681	23.801	26.7171	24.4751	24.4191	27.8091	25.2513	26.2234
			Score	**0.11**	**0.69**	**0.10**	**0.89**	**0.11**	**0.94**	**0.96**	**0.12**	**0.93**	**0.90**

Figure 11-11 – TOPSIS results with SAW & AHP optimals for Priority-based, per mode (volume x4)

				Options:									
				1	2	3	4	5	6	7	8	9	10
			Importance	AHP 70-31-31	70-37-25	80-36-36	80-47-25	90-41-41	90-56-26	SAW TOPSIS 90-57-25	100-46-46	100-67-25	110-76-26
Criteria:	1	Car	0.195	154.761	66.3939	147.033	37.9387	142.026	28.9561	26.3781	138.764	21.0892	19.5231
	2	Bus	0.297	113.661	57.8553	108.169	43.1752	104.654	41.6663	42.4612	102.399	52.7291	64.8794
	3	Bike	0.034	11.086	7.97658	12.3469	7.00866	13.6111	6.63231	6.25627	14.8776	5.65475	5.47129
	4	Ped	0.473	24.7245	23.4887	25.681	23.801	26.7171	24.4751	24.4191	27.8091	25.2513	26.2234
			Score	**0.13**	**0.72**	**0.12**	**0.90**	**0.12**	**0.93**	**0.94**	**0.13**	**0.87**	**0.77**

Figure 11-12 – TOPSIS results with SAW & AHP optimals for Priority-based, per direction (volume x4)